学位論文 (要約)

Optimization of gene therapy strategies for chronic granulomatous disease using patient autologous iPS cells

(患者由来人工多能性幹細胞を用いた遺伝子治療の至適化戦略)

Lin Huan-Ting

林　煥庭

Contents

Abbreviations

Ab antibody
ADA-SCID adenosine deaminase-deficient severe combined immunodeficiency disease
ALP alkaline phosphatase
Cas 9 CRISPR associated protein 9
CO codon optimized
CD cluster of differentiation
CGD chronic granulomatous disease
CRISPR clustered regularly interspaced short palindromic repeats
DHR dihydrorhodamine
DMEM dulbecco`s modificd eagle medium
DMSO dimethyl sulfoxide
ddPCR droplet digital PCR
EB embryoid body
EFS EF1α short
ESC embryonic stem cell
FACS fluorescence activated cell sorting
FBS fetal bovine serum
FCS fetal calf serum
FITC fluorescein isothiocyanate
G-CSF granulocyte colony stimulating factor
GT gene therapy
GvHD graft versus host disease
HIV human immunodeficiency virus
HPC hematopoietic progenitor cell
iPSC induced pluripotent stem cell
IRES internal ribosome entry site
LTR long-term repeat
MEF mouse embryonic fibroblast
MFI mean fluorescence intensity
MOI multiplicity of infection
MLV murine leukemia virus

MPO myeloperoxidase

MSC mesenchymal stem cell

NADPH nicotinamide adenine dinucleotide phosphate

NET neutrophil extracellular trap

NBT nitroblue tetrazolium

NTC no template control

PB peripheral blood

PID primary immunodeficiency

PMA phorbol 12- myristate 13-acetate

PURO puromycin

RFU relative fluorescence units

ROS reactive oxygen species

RT-PCR reverse-transcriptase polymerase chain reaction

SC single copy

SCGT stem cell gene therapy

SCID severe combined immunodeficiency

SFFV spleen focus forming virus

SIN self-inactivating

SOD superoxide dismutase

SVI single vector insertion

TALEN transcription activator-like effector nucleases

VCN vector copy number

VEGF vascular endothelial growth factor

WAS Wiskott-Aldrich syndrome

WG Wright Giemsa

XCGD X-linked chronic granulomatous disease

ZFN zinc finger nucleases

Abstract

Hematopoietic stem cell gene therapy (SCGT) has been successful in restoring cell functionality in monogenic hematological disorders. However, XCGD appears to be unique in that the appearance of functional neutrophils in the peripheral blood occurs only for a transient period. One previously unexplored possibility is that non-physiologically regulated "ectopic" expression of gp91phox may be detrimental to neutrophils. Since most of hematopoiesis occurs in the bone marrow, a suitable *in vitro* modeling system is required to investigate this hypothesis. In this study, integrating alpharetroviral vectors containing a ubiquitous promoter to drive the ectopic expression of codon optimized gp91phox cDNA were used to transduce XCGD-iPSCs. It was found that in the mature fraction of neutrophils differentiated from transduced XCGD-iPSCs, cellular recovery in terms of gp91phox expression and ROS production was abruptly lost before cells had fully differentiated on a per cell basis. Most critically, in the developing fraction, ectopic gp91phox expression could be identified but not in the controls. This corresponded with reduced cell viability and may be considered as an impediment towards further differentiation of developing neutrophils. Therefore affording cellular protection from the detrimental effects of ectopic gp91phox expression may improve XCGD clinical outcomes.

Chapter 1. Introduction

1.1 Historical background of chronic granulomatous disease

The first recorded cases were identified in 1954. Five children were suffering from recurrent infections and hypergammaglobulinemia but the cause was unknown. Years later, more cases with similar clinical presentations were found [1, 2]. "Granulomatous lesions" developed in the skin and visceral organs of these patients, which was to give the disease its modern name. Initially it was called "fatal granulomatous disease of childhood" as patients died within the first decade of life. Thereafter it was discovered that mortality rates could be greatly improved through the appropriate prophylactic and palliative treatment and this disease became simply known as chronic granulomatous disease (CGD). Eventually it was demonstrated that CGD is characterized by defective functionality in phagocytes [3] attributable to the impaired ability to produce reactive oxygen species (ROS) [4]. This severely compromises the antimicrobial activities of neutrophils in particular, leading to granuloma formation as foreign infectious organisms are successfully phagocytosed but not fully eliminated.

1.2 Epidemiology, clinical presentation and diagnosis

The prevalence rate of CGD is approximately 1 in 250,000 [5]. Patients are particularly susceptible to recurrent infections with bacteria such as *Staphylococcus* and *Pseudomonas* as well as fungal infections most commonly with *Aspergillus*. Symptoms range from pneumonia to abscess formation in skin or visceral organs. Granulomas can form in the respiratory, digestive and urinary tracts to a point where it becomes painful and obstructive. Clinically CGD is diagnosed by demonstrating the absence of oxidase activity in phagocytes. This may be confirmed by one of two ways through either the nitroblue tetrazolium dye reduction (NBT) test [6] or the dihydrorhodamine (DHR) assay [7]. Generally speaking, CGD patients require lifelong prophylactic treatment in the form of intravenous broad-spectrum antibiotic or antifungal drug therapy. Patient prognosis can be much improved by early diagnosis however, mortality rates remain unacceptably high approaching 5% annually and only 21% of patients live beyond the age of seven [8].

1.3 NADPH oxidase

Nicotinamide adenine dinucleotide phosphate-oxidase (NADPH) oxidase is a multicomponent enzyme complex the impaired functioning of which gives rise to the characteristic CGD phenotype. The membrane portion of this complex consists of two subunits gp91phox and p22phox together forming a heterodimer complex also known as flavocytochrome b_{558}. It is worth noting is that the stability of either protein is dependent on being in the dimerized assembled form. The remaining components p47phox, p67phox, p40phox also exist in a complex [9] and are found in the cytoplasm alongside Rac2. In the resting state, NADPH oxidase is in an unassembled state consisting of the membrane bound flavocytochrome$_{b558}$ and cytosolic components. Upon stimulation by an inflammatory stimulus such as opsonized microorganisms, the active complex is rapidly assembled. The entire intracellular component including Rac2 translocates to the membrane and interacts with flavocytochrome$_{b558}$ (Figure 1).

1.4 Reactive oxygen species and the "respiratory burst"

Functionally speaking NADPH oxidase acts as an electron transport system in a cascade sequence of events (Figure 2) commonly referred to as the "respiratory burst." Firstly, a single reduced electron is transported across the plasma membrane extracellularly by the activated complex in which a single oxygen molecule (O_2) is converted into a superoxide ion (O_2^-). This molecule is highly unstable and is rapidly converted into hydrogen peroxide by the action of superoxide dismutase (SOD). Hydrogen peroxide is then converted to water and molecular oxygen at the end of this series of reactions. Collectively these highly reactive and unstable molecules are called reactive oxygen species (ROS), which is critical to neutrophil functionality. It is important to note that it is not the ROS themselves per se that kills engulfed pathogens. Intracellularly, different types of granules are found within neutrophils that contain enzymes with antipathogenic activity [10]. Upon phagocytosis, ROS permits the fusion of the granular membrane and that of the phagolysozome thus releasing the enzymes into the extracellular space [11]. ROS is also critical to the formation of neutrophil extracellular traps (NETs), which is involved in the extracellular killing of pathogens [12].

1.5 Molecular defects

Absent expression or defective activity in any of the NADPH oxidase subunits can lead to the development of the classic CGD phenotype [13]. The encoding genes are found in different chromosomes with considerable variation in the prevalence of mutations occurring at these locations (Table 1). The most prevalent and severe form is X-linked CGD (XCGD), which results from defects with the *CYBB* gene located on the X chromosome encoding for the gp91phox subunit of NADPH oxidase. Approximately 65% of male CGD patients suffer from the X-linked form of the disease. However, carrier XCGD females may also display some of the disease symptoms depending on the percentage of circulating neutrophils that are functional. This may vary from one individual to another but it is thought that the presence of approximately 10% in functional circulating cells would be sufficient for female carriers to remain relatively healthy [14]. In addition, there are rare cases of individuals presenting with a "split-phenotype" in which a "loss of function" mutation occurs whereby protein expression of gp91phox is normal but oxidase activity is either very low or absent [15]. In another case, a patient presented with a unique mutation in the *CYBB* gene resulting in severely compromised functionality in neutrophils but residual oxidase activity could be detected in monocytes/macrophages, which drastically reduced the susceptibility to infections [16]. For the majority of cases however, both the expression of corresponding protein attributed to the mutation and ROS production is completely absent.

1.6 Non-curative treatment for CGD

For almost all patients of CGD regardless of the underlying molecular defect, lifelong prophylaxis is usually required. Depending on the type of infection contracted, the strategy may include one, or a combination of both antimicrobial and antifungal medication such as cotrimoxazole and itraconazole [17] respectively. In selected cases, interferon-gamma (IFN-γ) may also be administered to patients. Although the precise underlying mechanism is unclear, it is known that IFN-γ may partially restore oxidase activity in those with the X-linked form (XCGD, gp91phox deficiency) of the disease [18]. There are also known examples where surgical intervention is required to relieve obstruction of the respiratory, gastrointestinal and urinary tracts that occur as a result of granuloma formation. Focal points of infection that appear refractory to chemical prophylaxis and where an abscess has developed may also require surgical drainage.

In any case, none of these treatments are curative and as such there remains the risk of developing a fatal infection.

1.7 Hematopoietic stem cell gene therapy

In terms of a curative treatment for CGD, without any gene manipulation, the preferred choice would be allogeneic transplantation of bone marrow cells from a healthy HLA-matching donor. The therapeutic concept behind it is for healthy donor hematopoietic stem cells (HSCs) can reconstitute life-long hematopoiesis in a recipient patient [19]. Where a matching donor cannot be found then hematopoietic SCGT remains the only solution of offering a permanent cure to CGD. This treatment involves genetic manipulation of autologous HSCs, in the form of G-CSF stimulated PB $CD34^+$ cells, which is subsequently infused back into the patient to achieve long-term and sustained expression of a defective protein in all hematopoietic lineages and to restore cell functionality. Most commonly gene replacement is achieved by inserting a therapeutic transgene into the host genome by using a viral vector as a delivery vehicle. The natural infectious properties of viral vectors means that therapeutic genes are delivered into target cells with greater efficacy. Integrating vectors tends to be preferred as integration into the host genome is likely to lead to more sustained gene expression. Further modifications can be made to maximize this efficiency such as a desired promoter of choice or pseudotyping the virus with specific envelope proteins. Specifically with regards to hematopoietic SCGT, gammaretroviral vectors based on the murine leukemia virus (MLV) and lentiviral vectors based on the human immunodeficiency virus (HIV) have been commonly used. Both are integrating vectors that have been shown to be capable of achieving long-term transgene expression *in vivo*. To harness this technology, a number of important safety features have been necessary. Vectors are designed such that they are replication incompetent through removal of viral replication genes or those that are necessary for budding from the host cell. Viral promoter and enhancer elements found in the LTR may cause undesired transcriptional effects on the host genome. Vectors therefore have a self-inactivating design (SIN) in which transcriptional enhancers and promoters in the 3` LTR are deleted. The same modifications are copied onto the 5` LTR following one round of vector replication thus the provirus becomes inactive [20]. Unfortunately insertional mutagenesis is an inherent risk of using vector mediated

gene therapy. Although some are though to have a more neutral profile, this cannot be avoided by design alone.

1.8 CGD clinical trials

In the clinic, most of the attempted cases have been the X-linked form of the disease. Unfortunately XCGD is commonly known as the *"engraftment dilemma."* This is because hematopoietic SCGT has been demonstrated to be effective for treating other PIDs such as adenosine deaminase-deficient severe combined immunodeficiency disease (ADA-SCID) [(21)], SCID-X1 [(22)] and Wiskott-Aldrich syndrome (WAS) [(23)]. For CGD however, the appearance of gene-marked, and therefore functional neutrophils appear to be transient only and very quickly falls to almost negligible levels after a few months. This is despite high initial numbers of transplanted and gene-marked cells [(24)]. Initially these unfavorable outcomes were attributed to the primitiveness of vector designs and the avoidance of myelosuppression [(25)], which is particularly undesirable especially in treating young children. Thereafter clinical protocols were amended with the inclusion of myelosuppresion and the use of strong ubiquitous promoters such as that derived from the spleen focus-forming virus (SFFV) to drive gp91phox expression [(26)]. Much higher levels of transduction efficiency could be achieved with significantly higher levels of gene marking in the peripheral blood (PB). Unfortunately this came at the cost of undesired insertional activation of the EVI1-MDS1 proto-oncogene leading to myelodysplasia with monosomy 7 [(27)]. For these reasons, ongoing attempts at improving XCGD gene therapy in particular have been focused largely upon minimizing the genotoxic risk but with limited progress in achieving higher and more sustained levels of gene marking in the myeloid compartment.

1.9 The potential for gp91phox toxicity

Contrary to established thinking, it is reasonable to postulate that constitutive expression of a therapeutic transgene may not entirely be beneficial. In hematopoietic SCGT, integrating viral vectors containing a ubiquitous promoter to drive transgene expression are commonly used. In the context of XCGD, it means the possible constitutive expression of ectopic gp91phox in non-targeted cell populations even within the same path of myeloid differentiation. This non-physiologically regulated expression of ectopic gp91phox could result in perturbations in ROS production

leading to unknown detrimental effects. It has been reported that raised intracellular levels of ROS (mitochondria derived) could negatively compromise the functionality of HSCs [28]. However, this may not be fully attributable to vector mediated constitutive overexpression of gp91phox, which is stable only in the assembled form with other NADPH oxidase subunits [29]. In HSCs, these subunits are produced in much lower amounts compared with mature phagocytes [30], which may be insufficient to fully support stable enzyme assembly through incorporating transgene-derived gp91phox protein. However, once differentiating cells become phagocytes such as neutrophils, there is greater possibility that NADPH oxidase-mediated perturbations in ROS production could result in the occurrence of detrimental effects secondary to ectopic gp91phox expression

1.10 Stem cells and the need for pluripotency

Stem cells are defined as cells with the ability to "self-renew", meaning that they can undergo cycles of mitotic division whilst maintaining the same undifferentiated state as the parent cell and having the unique characteristic of "potency", which is the capacity to differentiate into other cell types. Cells can be characterized into a hierarchical system based on potency with cells of the "morula" being the most potent (Figure 3). In adult individuals, only multipotent and oligopotent stem cells can be found *in vivo*. It is though that the multipotent cells such as HSCs and EpiSCs may have some potential applications in regenerative medicine through direct transplantation by replacing these populations. However, the prospective isolation and expansion of these cells continues to remain a technical challenge. For these reasons, efforts began to move towards searching for cells higher up in the hierarchical order of potency. Embryonic stem cells (ESCs) were thought to be an attractive target because they are pluripotent, meaning that theoretically they can be induced to differentiate into almost any somatic cell type. In terms of transplantation medicine, there are potential dangers in unwanted teratoma formation or the possibility of eliciting an immune response. The most difficult problem is the ethical concerns associated with the establishment of ESCs *in vitro*, which necessitates the destruction of a fertilized embryo.

1.11 Induced pluripotent stem cells and disease modeling

In 2006, the group of Prof. Shinya Yamanaka reported the first successful generation of mouse iPS cells [31], which was followed one year later by human iPS cells [32]. Pluripotency may be defined as "an unlimited ability to give rise to all cell of the embryo" [33]. Although there are fundamental differences between ESCs and iPSCs, for the most part, they are considered to be equivalent as both are pluripotent but with iPSCs, there are no accompanying ethical concerns relating to fertilized embryo destruction. When subjected to the teratoma assay, both cell types can contribute to tissue from all three germ layers. It is now also possible to reprogram different somatic cell targets such as hematopoietic cells, adipocytes or hepatic progenitor cells into pluripotency (Figure 4). One of the most valuable features of iPS cells is in its application in disease modeling and offering more personalized therapy to patients [34]. By reprogramming somatic cells from a patient to pluripotency, the same genetic defect is retained. This allows various disease phenotypes to be recapitulated *in vitro*. In the field of gene therapy, this could be particularly useful because up till now, disease modeling replied upon the use of animal models or immortalized cell lines whereby the physiological relevance to the *in vivo* situation in patients is questionable. Most of hematopoiesis occurs within the bone marrow with only mature blood cells released into the bloodstream. Using iPSCs, there is also the additional advantage that *in vitro* differentiation may be controlled by cytokines, allowing for the identification of the precise point of origin from which pathological features arise. However, thorough validation is required as to whether cells derived under artificial conditions can become reliable representations of *in vivo* development.

It is known that monogenetic hematological disorders such as CGD is particularly suited to disease modeling using patient autologous iPSCs. This method is particularly useful in elucidating the underlying pathophysiology of the disease and understanding the correlation between transgene expression and functional recovery. In terms of physiological relevance, the preferred *in vitro* modeling system to investigate hematological disorders would be to use $CD34^+$ cells from patients. For reasons of practicality however, these cells can be difficult to obtain repeatedly, therefore making it challenging to study the differentiation process intensely, which would allow possible impediments to differentiation to be identified. In relation to CGD, there have already been a number of proof-of-principal studies demonstrating

the feasibility of using iPSCs to model and recapitulate the disease phenotype [34-36]. However, there has yet to be an attempt at identifying and evaluating a particular element of the underlying pathophysiological mechanism that may be unique to CGD and at least partially explain the lack of positive outcomes observed in CGD clinical trials.

1.12 Summary

It remains the case for XCGD that the appearance of functional cells in the peripheral blood following hematopoietic SCGT is only transient. This is despite similarities in vector design and conditioning regimens compared with other PIDs. It suggests that there could be elements of the underlying pathophysiology that may be considered unique to CGD.

1.13 Aims and objectives

The main goal is to establish a reliable disease model that can accurately recapitulate neutrophil differentiation and the XCGD phenotype *in vitro*. Integrating alpharetroviral vectors containing a ubiquitous promoter to drive gp91phox expression will be used to transduce XCGD iPSCs. Also, it will be necessary to know the precise number of provirus insertions in order to be able to accurately correlate transgene expression with functional recovery. As such the following points were identified as the main objectives for this study:

- Establish a reliable disease model using patient autologous iPS cells to model XCGD.
- Correlate the relationship between gp91phox expression and ROS production in neutrophils.
- Establish a simple and accurate method of estimating vector copy numbers in transduced cells.
- Determine the effect(s) of constitutive ectopic expression of gp91phox.

Chapter 2. Materials and methods

2.1 Sendai Virus (SeV) vectors

The design and development of non-integrating Sendai virus vectors harboring human *OCT3/4, SOX2, KLF4,* and *c-MYC* is as previously described [37]. Lipofectamine RNAi Max (Invitrogen, Thermo Fischer, Massachusetts, USA) to transfect established iPSC lines with small interfering RNA L527 to remove SeV vectors.

2.2 Alpharetroviral vectors

Alpharetroviral vectors [38] were kindly provided by Dr. Axel Schambach (Hannover Medical School, Germany). The production of viral supernatant is as previously described [39]. To construct the pAlpha.SIN.SFFV.IRES.PURO transfer plasmid, IRES-PURO (SalI-XbaI) from LV.EF.L3T4.IRES.PURO (provided by Dr. T. Yamaguchi, University of Tokyo, Japan) was cloned into pAlpha.SIN.SFFV.gp91s.oPRE. For pAlpha.EFS.IRES.PURO, the EF1α short promoter (NotI-BamHI) from pAlpha.EFS.gp91s.oPRE was cloned into pAlpha.SFFV.IRES.PURO. For the construction of pAlpha.SIN.EFS.gp91s.F2A.PURO.T2A.ΔLNGFR, there was initial PCR-amplification of gp91s (BamHI-ClaI) from pAS.SFFV.gp91s.oPRE, Puromycin resistance gene (XbaI-BspEI) from CS.CDF.CG.PRE [40] and ΔLNGFR (HpaI-AccI) from SFCMM-2 [41]. These three fragments were then cloned into T7 mOKS [42] to replace Oct4, Klf4 and Sox2 respectively to create pT7.gp91s.PURO.ΔLNGFR. From this, the gp91s.F2A.PURO.T2A.ΔLNGFR cassette (BamHI-AccI) was then cloned into pAlpha.EFS.gp91s.oPRE. For the control vector pAlpha.EFS.PURO.T2A.ΔLNGFR.oPRE, the PURO.ΔLNGFR cassette (BamHI-AccI) from T7.gp91s.PURO.ΔLNGFR was inserted instead.

2.3 Generation of patient autologous iPSCs and transduction

Peripheral blood samples were obtained from either a healthy volunteer or a XCGD patient on informed consent by following the Declaration of Helsinki standard ethics procedure with approval from the Institutional Ethical Committees. PB $CD34^+$ cells were isolated using the CD34 MicroBead Kit according to the manufacturer's protocol (Miltenyi Biotec, Bergisch Gladbach, Germany). Isolated cells were then transduced with the earlier described SeV vectors to generate iPSCs, which were

maintained under conditions as previously described [43]. For the transduction of iPSCs from either an XCGD or healthy genetic background, cells were first maintained under feeder free conditions on matrigel™ (BD Biosciences, New Jersey, USA). Transduced cells were subsequently maintained on puromycin resistant mouse embryonic fibroblasts (MEFs) under constant puromycin (A11138-03, Life Technologies, Thermo Fischer, Massachusetts, USA) selection pressure.

2.4 Immunocytochemical staining of iPSCs

To begin with, iPSC colonies were fixed using 5% paraformaldehyde and permeabilized with 0.1% Triton X-100. Primary phycoerythrin (PE)-conjugated anti-SSEA-4 antibody (FAB1435P, R&D Systems, Minneapolis, USA) was used for SSEA-4 staining. For TRA-1-60 and TRA-1-81, pretreated colonies were incubated with primary mouse anti-human TRA-1-60 (MAB4360, Merck Millipore, Massachusetts, USA) and mouse anti-human TRA-1-81 (MAB4381, Merck Millipore, Massachusetts, USA). This is followed by incubation with secondary Alexa Fluor 488-conjugated goat anti-mouse antibody (A11029, Molecular Probes-Invitrogen, Thermo Fischer, Massachusetts, USA). 4',6-diamidino-2-phenylindol (DAPI, Roche Diagnostics, Basel, Switzerland) were used to counterstain cell nuclei.

2.5 Alkaline phosphatase activity in iPSCs

10% Formalin Neutral Buffer Solution (Wako, Tokyo, Japan) was used for the fixation of iPSC colonies. Alkaline phosphatase activity was then detected using the 1-Step™ NBT/BCIP (34042, Thermo Fischer Scientific, Massachusetts, USA) solution.

2.6 Teratoma Formation

A single cell suspension of dissociated iPSCs were injected at a density of 1.0 x 10^6 cells into the medulla of a single testis of a NOD/ShiJic-scid mouse [44]. After 12 weeks, the resulting teratomas were resected and then fixed in 5% paraformaldehyde before being embedded in paraffin. Microscopic sections were stained with hematoxylin and eosin (H&E) stain to determine evidence of tri-lineage germ layer contribution. Approvals for conducting these experiments were granted by the institutional regulation board for human ethics at the Institute of Medical Science, University of Tokyo.

2.7 Karyotyping and point mutation sequencing

Chromosome karyotyping (Q-banding) was performed by Chromosome Science Labo Inc. (CSL, Sapporo, Japan). 50 total metaphases were examined.

2.8 Extraction of genomic DNA

For PLB and iPS cells, genomic DNA was extracted using the NucleoSpin® Tissue XS kit (Takara, Shiga, Japan) as per manufacturer's instructions.

2.9 Estimation of the concentration of the target transgene by ddPCR

A final reaction mixture of 20ul volume was assembled consisting of the recommended 2x supermix, primers (forward and reverse, 1000nM final), probe stock solution and the stated amount of sample gDNA. The sample mixture was then transferred to a DG8™ cartridge and then placed into a QX200™ droplet generator (BIO-RAD, California, USA). Sample droplets were then transferred onto a 96-well PCR plate and then sealed using the PX1™ PCR Plate Sealer (BIO-RAD, California, USA). The C1000 Touch™ Thermal Cycler (BIO-RAD, California, USA) was used to amplify droplets to end point under the following conditions 95°C for 10 minutes followed by 40 cycles of 94°C for 30 sec, 54°C for 120 sec with a final heating step of 98°C for 10 minutes and then held at 4°C. The plate is then placed into a QX200™ droplet reader (BIO-RAD, California, USA) to determine positive and negative droplets and then using the manufacturer's QuantaSoft software. The concentration of the target amplicant from each sample is estimated for both the target and the RPP30 reference gene. The estimation of VCN can then be calculated by dividing twice the concentration of the target species by the concentration of the reference species.

2.10 Neutrophil differentiation of human iPSCs

Human iPSCs were first differentiated into hematopoietic progenitor cells as previously described [45] with slight modifications. In brief, irradiated puromycin resistant C3H10T1/2 were co-cultured with detached iPSC colonies in hematopoietic cell differentiation medium (Iscove's modified Dulbecco's medium supplemented with 15% fetal bovine serum [FBS] and a cocktail of 10 mg/ml human insulin, 5.5 mg/ml human transferrin, 5 ng/ml sodium selenite, 2 mM L-glutamine, 0.45 mM a-monothioglycerol, and 50 mg/ml ascorbic acid in the presence of VEGF) under sustained puromycin selection pressure. On day14, hematopoietic progenitor cells

(HPCs) were harvested from "sac-like" structures. For neutrophil differentiation, HPCs were continuously co-cultured with irradiated C3H10T1/2 cells in differentiation medium (αMEM + 10%FBS [Biological Industries, Kibbutz Beit Haemek, Israel] + 1% PSG) including 50 ng/ml G-CSF (R&D Systems, Minneapolis, USA) with a half medium change every 3 days.

2.11 Cell morphology and expression of cytoplasmic proteins

After methanol fixation, cell morphology of differentiated neutrophils were determined by Wright-Giemsa (WG) staining using Hemacolor® solution 2 (Red, 111956) and solution 3 (Blue, 111957) (Merck Millipore, Massachusetts, USA). Myeloperoxidase and alkaline phosphatase were stained using the New PO-K and alkaline phosphatase staining kits respectively (MUTO PURE CHEMICALS, Tokyo, Japan).

2.12 NBT-coated yeast phagocytosis assay

Autoclaved Baker yeast was suspended at a density of $1x10^8$/mL in 0.5% NBT solution (Sigma-Aldrich, St. Louis, USA) dissolved in phosphate buffered saline (PBS). A 5 µl suspension was incubated with $2.5x10^5$ differentiated neutrophils suspended in 50 µl of FBS. After 1 hour of incubation at 37°C with periodic tapping, cytospin preparations were made of each sample, which was then stained with 1% safranin-O (MUTO PURE CHEMCALS, Tokyo, Japan).

2.13 Formation of neutrophil extracellular traps

Differentiated neutrophils were seeded onto poly-L-lysine (Sigma-Aldrich, St. Louis, USA) coated glass coverslips (Matsunami, Osaka, Japan). The method used for generating neutrophil extracellular traps were adapted from a previously described protocol [(46)]. After permeabilization and fixation, cells were stained with primary purified polyclonal anti-MPO antibody (Abcam, Cambridge, UK) and then secondary Alexa Fluor 546-conjugated goat anti-rabbit antibody (A11029, Molecular Probes-Invitrogen, Thermo Fischer, Massachusetts, USA) along with SYTO®13 (Life Technologies, California, USA) to stain nucleic acids.

2.14 Flow cytometry determination of surface marker and NGFR expression

For surface staining, cells were first stained with primary monoclonal rabbit anti-human FCGR1A antibody (EPR4623, Abcam, Cambridge, UK). This was followed by secondary Alexa Fluor 488-conjugated goat anti-rabbit antibody (A11034, Molecular Probes-Invitrogen, Thermo Fischer, Massachusetts, USA) and BV605-conjugated anti-human CD15 (W6D3, BioLegend, California, USA). Where the detection of NGFR expression was subsequently desired, cells are then treated with FcR blocking reagent (130-059-901, Miltenyi Biotec, Bergisch Gladbach, Germany). This was followed by staining with primary anti-CD271 (NGFR) (HE20.4, Biolegend, California, USA) and then secondary APC/Cy7-conjugated goat anti-mouse IgGI (Southern Biotech, Birmingham, USA) or BV421-conjugated anti-mouse IgG (RMG1-1, Biolegend, California, USA). Data were acquired on FACSAria™ I or II sorter (BD Biosciences, New Jersey, USA) and analyzed using FlowJo X software (Tree Star, Oregon, USA).

2.15 Intracellular detection of gp91/p47/p67 phox

Following surface staining of CD64 and CD15, cells were fixed and permeabilized using the Fixation/Permeabilization solution (Becton Dickinson, New Jersey, USA). For the detection of gp91phox, cells were then stained with PE-conjugated monoclonal anti-human gp91phox antibody (7D5, MBL, Nagoya, Japan) or control PE-conjugated anti-mouse IgG1 (Biolegend, California, USA). Alternatively, cells were instead incubated with anti-p47phox (clone 1, Becton Dickinson, New Jersey, USA), anti-p67phox mAb (clone D-6, Santa Cruz Biotechnology, California, USA) or purified mouse IgG1 (Becton Dickinson, New Jersey, USA). This was followed by reaction with PE- conjugated anti-mouse IgG1 (Southern Biotech, Birmingham, USA).

2.16 Detection of reactive oxygen species

The production of reactive oxygen species by test cells including peripheral blood, and differentiated developing and mature neutrophils was detected using the dihydrorhodamine123 (DHR) flow cytometry assay as previously described [(7)]. In brief, cell samples were suspended in ~400 µl of reaction buffer (HBSS + 0.5% BSA). Catalase (Sigma-Aldrich, St. Louis, USA) was added at a final concentration of 1400 U/µL alongside 1.8µl of a 29 mM stock solution of DHR (Sigma-Aldrich, St. Louis,

USA). Phorbol myristate acetate (PMA; Sigma-Aldrich, St. Louis, USA) was added to stimulate samples at a final concentration of 0.2 μmol/l. After 15-minute reaction at 37°C, the samples were washed and analyzed by flow cytometry. Where indicated, cell surface antigen was stained as previously described.

2.17 Reverse transcription (RT)-PCR

The RNeasy Micro kit (Qiagen, Hilden, Germany) was used to extract RNA from iPSCs, which was then reverse transcribed using the High Capacity cDNA Reverse Transcription kit (Applied Biosystems, Thermo Fischer, Massachusetts, USA) with random 6-mer primers. RT-PCR was performed using ExTaq HS (Takara, Shiga, Japan). Individual PCR reactions were normalized against GAPDH rRNA. Primer sequences can be found in Table 2.

2.18 Intracellular detection of ER stress markers

Cells were first stained for CD64 and CD15 as followed by treatment with FcR blocking reagent (130-059-901, Miltenyi Biotec, Bergisch Gladbach, Germany). Cells were then treated with the Fixation/Permeabilization solution (Becton Dickinson, New Jersey, USA). Staining of ER-stress markers were done firstly with primary rabbit anti-human EIF2S1 (E90, Abcam, Cambridge, UK), rabbit anti-human BiP (C50B12), mouse anti-human phosphor SAPK/JNK (G9, CST, Masssachusetts, USA) and mouse anti-human XBP1 (S Isoform) antibodies. This was followed by secondary staining with either PE-conjugated mouse IgG1 (RMG1-1, Biolegend, California, USA) or goat anti-rabbit AF546 antibody (A11010, Molecular Probes-Invitrogen, Thermo Fischer, Massachusetts, USA). In the final step, detection of NGFR expression is as previously described.

2.19 Cell death apoptosis assay

Following cells surface and NGFR staining, cell viability was assessed using the PE Annexin V Apoptosis Detection Kit I (BD Pharmingen™, New Jersey, USA) as per manufacturer's instructions.

2.20 Statistical analysis

Mean grouped values were compared using one-way or two-way ANOVA. All statistical analyses were carried out using Prism 6 software (Graphpad, San Diego, USA).

2.21 PLB Cell maintenance

XCGD PLB-985 cells were generated from the immortalized PLB-985 myelomonocytic leukemic cells line by disruption of the CYBB gene encoding the gp91phox protein by homologous recombination [47]. Single copy (SC) PLB cells were kindly provided by Dr. Manuel Grez (Georg Speyer Haus, Frankfurt) is a clonal population containing only one copy of the provirus pAlpha.SIN.EFS.gp91s.oPRE. E91P and S91P PLB cells are transduced XCGD PLB-985 cells carrying the provirus insertions pAlpha.SIN.EFS.gp91s.IRES.PURO.oPRE and pAlpha.SIN.SFFV.gp91s.IRES.PURO.oPRE respectively. Cells were maintained in RPMI 1640 (Gibco) with 10% FBS and 1% PSG (Gibco). XCGD-iPSCs were generated and maintained as previously described.

Chapter 3. Results

3.1 Generation and characterization of XCGD iPSCs

$CD34^+$ cells were isolated by magnetic separation from the peripheral blood of an XCGD patient. Sendai virus vectors carrying the four Yamanaka factors were used for reprogramming into pluripotency. Within 30 days following transduction, embryonic stem cell (ESC)-like colonies could be identified (Figure 5). For all subsequent transduction and differentiation experiments XCGD iPSC (clone #8) was used. The following representative characterization data was generated using clone #8. It can be observed that XCGD iPSCs exhibited alkaline phosphatase (ALP) activity and displayed the surface markers SSEA-4, Tra-1-60 and Tra-1-81 (Figure 6a). XCGD-iPSCs could form teratomas consisting of tissues derived from the three germ layers (Figure 6b), confirming that these cells display typical features of pluripotent stem cells. Also, it can be confirmed that cells exhibited a normal karyotype (Figure 7a). Most importantly, the same exact point mutation that had been identified in the patient in the *CYBB* gene (c.1448G>A p.Trp483X) was successfully retained (Figure 7b). Therefore neutrophils differentiated from these unmodified XCGD iPSCs should display the same characteristic functional defects of the disease. XCGD iPSCs also expressed pluripotency genes as determined by RT-PCR (Figure 8).

3.2 Hematopoietic differentiation from pluripotent stem cells

To begin with, hematopoietic differentiation is initiated by adopting a co-culture system with irradiated C3H10T1/2 cells in the presence of VEGF. Over the course of the differentiation period, “sac-like” structures containing hematopoietic progenitor cells (HPCs) form on top of the feeder cells. After 14 days, HPCs can be harvested and further induced to undergo differentiation into mature blood cells. These HPCs are heterogeneous in composition. To assess their hematopoietic potential, $CD34^+Lin^-$ cells (Figure 9a) derived from either XCGD iPSCs or a healthy control line (healthy) were sorted and then subjected to the colony-forming assay in semi-solid culture. The total numbers of colonies were counted after 12 days (Figure 9b). Since all experimental groups can form colonies, it confirms the validity of this protocol in producing cells with hematopoietic potential.

3.3 Neutrophil differentiation and recapitulation of the XCGD phenotype

The differentiation process from HPCs to neutrophils requires an additional 5 to 7 days (Figure 10). A similar co-culture system with irradiated C3H10T1/2 cells is adopted except G-CSF is used for neutrophil differentiation. Initially, the differentiation protocol was optimized using iPSCs from a healthy donor (healthy) only. Differentiated neutrophils displayed the characteristic multi-lobed appearance of the nuclei following Wright Giemsa (WG) staining. Cells contained myeloperoxidase (MPO) and alkaline phosphatase (ALP), which are enzymes found in cytoplasmic granules the appearance of which corresponds with the increasing maturation status of neutrophils (Figure 11a). The ability of differentiated neutrophils to phagocytose infectious microorganisms was mimicked through the NBT-coated yeast assay [(48)]. Ingested NBT-coated yeast is purple/black in color due to NBT reduction by ROS (Figure 11b, white arrows). It has been reported that neutrophils can generate neutrophil extracellular traps (NETs), composing of nuclear constituents and granules for the extracellular killing of large pathogens [(49)]. Here NETs formed by iPSC-derived neutrophils can be visualized by staining for nucleic acids and MPO, a critical component of these structures [(50)] (Figure 11c, white arrows).

Clinically the characteristic XCGD phenotype is defined by the absence of any oxidase activity in neutrophils. This can be determined by using the DHR assay. Following PMA stimulation, differentiated neutrophils with a healthy genetic background produced ROS at levels comparable to that of peripheral blood neutrophils (Figure 12a). However, this was completely absent in neutrophils differentiated from XCGD-iPSCs, indicating that the XCGD phenotype has been successfully recapitulated in this modeling system (Figure 12b).

Within the differentiation culture, a heterogeneous population of developing ($CD64^{Dull}CD15^{Dull}$) and mature ($CD64^{High}CD15^{High}$) neutrophils could be identified. Following cell sorting, it can be seen that in the "mature" fraction, most of the population are either band or segmented neutrophils. In the "developing" fraction, cells have the appearance of either myelobalsts or myelocytes (Figure 13). In addition, to support the use of CD64 and CD15 expression to define neutrophil maturation status, it can be seen that CD66b, a surface adhesion molecule found on mature neutrophils [(51)], were more highly expressed (grey histogram) in mature

($CD64^{High}CD15^{High}$) neutrophils compared with developing neutrophils ($CD64^{Dull}CD15^{Dull}$) regardless of differentiation from either an XCGD or healthy genetic background (Figure 14).

3.4 CGD modeling using PLB cells

XCGD-PLB cells were generated from wild-type (WT) PLB cells in which there is targeted disruption of the *CYBB* gene such that there is no expression of gp91phox protein as previously described [47]. The single vector insertion (SVI) PLB cells contain only one single copy of the pAlpha.SIN.EFS.gp91s.oPRE provirus generated by transducing XCGD-PLB cells with a gp91phox transgene-containing vector [52]. PLB cells were induced to undergo granulocytic differentiation for 7 days using DMSO and differentiated cells could be identified by CD11b expression (Figure 15a). It was discovered that only WT-PLB cells showed significant expression of $gp91^{phox}$ (Figure 15b, top row). None were detected in XCGD-PLB cells and expression was not significant in SVI-PLB cells. This indicates that having a single copy of the provirus is not sufficient to restore gene expression to physiological levels. To determine the correlation between transgene expression and functionality, in the same experiment, cells were also subjected to the DHR assay. Similar to gp91phox expression, only WT-PLBs showed significant ROS production (Figure 15b, bottom row). It appears that ROS production does correspond with gp91phox expression however, there may be exist some kind of a threshold/impediment to full functional recovery.

3.5 Cell transduction using alpharetroviral vectors

A schematic of all alpharetroviral vector designs are shown (Figure 16). Where indicated, PLB or iPSCs (XCGD and healthy) were transduced using these vectors. For the assessment of cellular recovery in neutrophils, vectors (a) and (b) were used whereby within the transgene cassette, a puromycin resistance gene was linked to codon-optimized (CO) gp91phox by an internal ribosome entry site (IRES) element to confer puromycin resistance to transgene positive cells. These designs were modified with the addition of a second selection marker ΔLNGFR (truncated NGFR) linked by 2A peptides to identify transgene positive cells where the sustained use of puromycin selection is not possible. (c) gp91phox containing vector. (d) Control vector containing only puromycin resistance gene and ΔLNGFR.

3.6 Specificity of primer design allows for accurate detection of target transgene

(This section cannot be made public on the Internet for 5 years from the date of doctoral degree conferral because it is currently under review and has yet to be accepted for publication.)

3.7 VCN estimation in transduced PLB and iPS cells

(This section cannot be made public on the Internet for 5 years from the date of doctoral degree conferral because it is currently under review and has yet to be accepted for publication.)

(This section cannot be made public on the Internet for 5 years from the date of doctoral degree conferral because it is currently under review and has yet to be accepted for publication.)

3.8 Sensitive detection of target transgene even at very low concentrations of template within heterogeneous samples by cellular dilution

(This section cannot be made public on the Internet for 5 years from the date of doctoral degree conferral because it is currently under review and has yet to be accepted for publication.)

3.9 Determination of variability in VCN estimation with reducing concentrations of template gDNA

(This section cannot be made public on the Internet for 5 years from the date of doctoral degree conferral because it is currently under review and has yet to be accepted for publication.)

3.10 Optimum accuracy in VCN estimation is achieved by be pre-digestion with restriction enzymes

(This section cannot be made public on the Internet for 5 years from the date of doctoral degree conferral because it is currently under review and has yet to be accepted for publication.)

3.11 Incomplete cellular recovery in XCGD-iPSC-derived neutrophils following gp91phox transfer

In this study, alpharetroviral vectors were used to transduce XCGD or healthy iPSCs. Following optimization of the ddPCR method of estimating average VCN, a summary of all transduced iPSCs (XCGD or healthy genetic background) used in all subsequent experiments can be found (Table 7) alongside the exact provirus insertion found in each cell type. Transduced cells were maintained under constant puromycin selection pressure and differentiated into neutrophils using the aforementioned protocol. A multi-colored flow cytometry analysis technique was adopted to allow the assessment of cellular recovery within the same staining sample of either developing ($CD64^{Dull}CD15^{Dull}$) or mature ($CD64^{High}CD15^{High}$) neutrophils. In the untransduced XCGD group, differentiated neutrophils expressed neither gp91phox nor generated

ROS in clear contrast to mature neutrophils differentiated from untransduced XCGD iPSCs on a per cell basis. It was discovered in transduced XCGD neutrophils that whilst increased recovery in gp91phox expression corresponded with increased VCN from 1.01 to 9.25 (pAlpha.SIN.EFS.gp91s.IRES.PURO.oPRE, MOI 1 and 10, Table 7), the extent of recovery was incomplete on a per cell basis compared with the healthy control group (Figure 25, top row). Similarly the restoration in ROS producing capacity was also incomplete (Figure 25, bottom row).

Should transgene-derived gp91phox protein be successfully assembled into NADPH oxidase, the expression levels of other subunits are also expected to increase as an indication of gp91phox stability. In a separate experiment, the expression of gp91phox (Figure 26, top row) was correlated with that of p47phox (Figure 26, middle row) and p67phox (Figure 26, bottom row), which are two important intracellular components of NADPH oxidase. It was found that basal levels of p47phox and p67phox were expressed at a lower level compared with the healthy controls despite the absence of gp91phox expression, in the XCGD group. Unexpectedly, there was a further opposing decrease in the expression of these two subunits that appeared to correlate negatively with an increase in gp91phox expression. Alongside the observation of incomplete cellular recovery, together with this trend, it may suggest that transgene derived gp91phox expression could induce a detrimental cellular response.

3.12 Ectopic gp91phox expression leads to non-physiological expression of ROS

Similar with previous hematopoietic SCGT clinical trials, an internal ubiquitous promoter (EFS and SFFV) within an integrating vector is used to drive gp91phox expression. Taking this into consideration, the ectopic expression of gp91phox could occur in non-targeted developing neutrophil populations resulting in non-physiological consequences. Using the same multi-color analysis technique as described previously, cells were first assessed for gp91phox expression. In mature cells (Figure 27, top row), gp91phox expression was found in all except for the XCGD group. As an additional control, the alpharetroviral vector was modified by using the SFFV promoter, which is known to have stronger activity [(54)] in general than the EFS promoter in driving transgene expression. Surprisingly restoration of gp91phox expression in the SFFV group was lower compared with the EFS group on

a per cell basis. This may in part be attributed to the susceptibility of this vector to silencing in pluripotent stem cells [55]. In the developing fraction (Figure 27, bottom row), no gp91phox expression was detected in either one of the untransduced control groups including those differentiated from a healthy genetic background (XCGD and Healthy). However, in neutrophils differentiated from transduced XCGD iPSCs, gp91phox expression can now be observed in developing neutrophils (EFS and SFFV). In the context of this study, the expression of gp91phox in this cell fraction is herein defined as "ectopic." Thereafter, cells were assessed for the generation of ROS firstly in the mature fraction (Figure 28, top row). As expected in the transduced groups (EFS and SFFV), ROS production was incomplete on a per cell basis compared with the healthy control. In the developing fraction (Figure 28, bottom row), no, or only marginal oxidase activity was detected in the untransduced controls (XCGD and Healthy). However, ROS production could now be detected in the developing fraction of the transduced groups, which may be described as "non-physiological" (EFS and SFFV). Therefore, a more refined hypothesis could be made that ectopic gp91phox expression in the developing fraction of neutrophils leads to non-physiological ROS production. This could result in the occurrence of detrimental effects that could impede further differentiation such that those cells that are able to transit into a mature hierarchy cellular recovery is incomplete.

3.13 Hierarchical transition of neutrophil differentiation

Should detrimental effects occur in developing neutrophils, it is plausible to think that this will imped further differentiation into mature neutrophils. To demonstrate that within this culture system, differentiating neutrophils could make the transition from developing to a mature hierarchy, after sac harvest, HPCs were differentiated for 3 days to obtain a heterogeneous mixture of both developing and mature neutrophils (Figure 29, Pre-sorting). At this point, the developing fraction ($CD64^{low}CD15^{low}$) was sorted and checked for purity in composition (Figure 29, Purity). Following an additional two days of differentiation, both developing ($CD64^{low}CD15^{low}$) and mature ($CD64^{High}CD15^{High}$) populations could be identified regardless of whether cells were differentiated from XCGD or healthy iPSCs (Figure 29, Differentiated). This confirms that in this culture system, cells follow this pathway of differentiation.

3.14 Raised expression in ER stress markers by developing neutrophils ectopically expressing gp91phox

To date, there have been no direct reports to suggest that perturbations in ROS homeostasis may be detrimental to neutrophils. It has been reported that ROS could induce ER stress [(56)], which would lead to cell death should levels remain elevated [(57)]. Since ectopic gp91phox expression leads to non-physiological ROS production in developing neutrophils, it is possible to speculate that ER stress levels may be elevated in these cells. To determine this, puromycin selection pressure was removed after HPC harvest from iPSC sacs, which may otherwise act as an additional factor that may be detrimental to cell viability. For this reason, the design of alpharetroviral vectors was further modified to include a truncated non-signaling version of the neural growth factor receptor (NGFR) (Figure 16c and 16d) the expression of which would represent transgene positive cells. The control vector however contains only puromycin resistance gene and NGFR.

The expression of the ER stress markers GRP78, pEIF2α, pJNK and XBP-1 were determined. Relative expression was calculated by subtracting the MFI of each marker in the NGFR -ve fraction from the NGFR +ve fraction (Figure 30). It was found that there was a statistically significant increase in GRP78 expression in the XCGD group (Figure 31a, XCGD, Ectopic gp91 vs. Control), whilst increased expression of pEIF2α occurred in healthy cells ectopically expressing gp91phox (Figure 31b, Healthy, Ectopic gp91 vs. Control). No statistically significant differences could be detected for pJNK and XBP-1 (Figure 31c and 31d). Although the effects of ectopically expressing gp91phox appears to be different in either healthy or XCGD cells, it is possible that an increased propensity for undergoing apoptosis is the end fate for these cells. Although it cannot be concluded that non-physiological ROS production can induce ER-stress, the data do suggest that these cells may have the propensity for undergoing such a fate. Therefore cell viability was determined in cells ectopically expressing gp91phox but given the wide range of physiological functions of NADPH oxidase, it is possible that perturbations in ROS production may lead to other effects.

3.15 Developing neutrophils ectopically expressing gp91phox are susceptible to increased cell death

Developing neutrophils were subjected to the 7-AAD/Annexin V apoptosis assay to determine their viability. The same groups of transduced XCGD and healthy iPSCs used in the ER-stress experiment was used here. Cell viability was determined as the total percentage of cell death, which was calculated by combining the total percentage of 7-AAD +ve only and 7-AAD/AnnexinV double positive cells (Figure 32) in both the NGFR -ve and NGFR +ve fractions. It was found that NGFR +ve developing neutrophils differentiated from iPSCs transduced with the gp91phox-containing vector exhibited more prominent levels of cell death compared with the NGFR -ve fraction. The same profile of cell death could be observed regardless of whether gp91phox was ectopically expressed in differentiated from either an XCGD (Figure 33a) or healthy (Figure 33b) background. These findings suggest that ectopic gp91phox expression can exert detrimental effects by subjecting developing neutrophils to an increased propensity for undergoing cell death, which may act as an impediment to further differentiation.

Chapter 4. Discussion

This study attempted to identify and evaluate a pathophysiological feature that may be unique to XCGD in the form of reduced viability in neutrophils occurring secondary to ectopic gp91phox expression. A disease model was established using patient autologous XCGD iPSCs. In addition, a multi-colored flow cytometry analysis technique was optimized, which allowed for the concomitant identification, within the same differentiation culture, of cells according to their maturation status (developing or mature) followed by other subsequent analyses. An emerging technique known as digital droplet PCR (ddPCR) was used for the simple yet accurate estimation of the average vector copy numbers in transduced cells. Overall, the main finding was that ectopic gp91phox expression occurred in non-targeted cell populations when a ubiquitous internal promoter was used. Indeed, it was demonstrated that ectopic gp91phox expression and non-physiological production of ROS occurred in developing neutrophils only in those differentiated from gp91phox-transduced XCGD-iPSCs. These cells also showed reduced viability regardless of an XCGD or healthy genetic background. Also, developing neutrophils could be demonstrated to make the hierarchical transition into mature cells. It suggests that ectopic gp91phox expression may act as an impediment to differentiation by raising the susceptibility to cell death of developing neutrophils.

Monogenetic diseases such as CGD are particularly suitable for disease modeling using iPSCs because of the relative ease with which the disease phenotype could be recapitulated *in vitro* and correlated to a defective gene. Prior to the development of iPSC technology, the main *in vitro* model available for XCGD were established by targeted disruption of gp91phox expression in wild type PLB-985 cells [(58)]. However, the extent of similarity of this system to the *in vivo* scenario can be questionable. Most notably, the mechanism of DMSO induced granulocytic differentiation remains unclear and is not a part of normal granulocyte differentiation. It is also known that these cells have bi-lineage differentiation potential [(59)], meaning that they could become either monocytes or neutrophils thus making a differentiation culture heterogeneous in composition. CD11b is the only surface antigen available to confirm differentiation but both populations of granulocytic cells express it. Still, it was deemed useful to attempt granulocytic differentiation and to optimize various

analyses protocols given their relative ease in maintenance. It was surprising to discover that SVI-PLB cells containing only a single vector insertion did not show significant expression of gp9phox or ROS production even following differentiation. From this unexpected result, there appeared to exist some kind of a "threshold" or limitation to gp91phox expression and the subsequent recovery in ROS production such that the detected levels are far below that found in the WT controls, which in further comparisons were not comparable with PB neutrophils (data not shown). This may be pointing to an inherent limitation of this modeling system. The next step was to further delineate the relationship between transgene expression and functional recovery in a more physiologically relevant model such as iPSCs. More specifically, it would be important to determine whether any positive effects may be observed by increasing the number of provirus insertions.

Most previous reports of hematopoietic differentiation from XCGD-iPSCs went through an intermediate embryoid body (EB) approach. This study is the first to demonstrate neutrophil differentiation utilizing the "sac" method because of the greater quantities of hematopoietic progenitor cells (HPCs) that can be harvested. The HPCs were demonstrated to have the potential to form colonies in semi-solid culture. However, a common weakness of both methods is the uncontrolled variability that exists in the physical size of both the EBs and sacs, which has been postulated to have an impact on the composition in terms of immunophenotype of the HPCs. Indeed, within each "sac" there exists a microenvironment for differentiation, which may be resistant to external cytokine manipulation. Prior to initiating neutrophil differentiation, there was no purification of HPCs beforehand. Given the heterogeneous composition, although it was found that there were committed progenitor cells of non-granulocytic lineages present, it was determined that these were minor in population size (data not shown) and thus would not compromise subsequent analyses. Recently a new protocol has been published of mimicking hematological differentiation through mesodermal development by single cell culture of pluripotent stem cells [(60)] under feeder free conditions, which may serve to minimize any variability. It was reported that key to initiating hematopoietic differentiation was to allow attachment of pluripotent cells to extracellular proteins found within the bone marrow. An adaptation of this protocol in the future may reduce some of the variability observed in this study.

In terms of neutrophil differentiation, it was demonstrated that external supplementation of G-CSF alone in the same C3H10T1/2 co-culture system was sufficient to generating mature neutrophils, which displayed the characteristic features of PB neutrophils. The reliability of this protocol was thoroughly validated using ESCs as well (data not shown). Worth mentioning is that this is the first study to demonstrate the formation of NETs by differentiated neutrophils *in vitro*. It is known that these critical structures for facilitating extracellular killing of microbes can only be formed by cells with normal capacity to generate ROS. Nonetheless, the most physiologically relevant assay for validating the functionality of differentiating neutrophils would be through *in vivo* testing. Still, within the outlined parameters of this study, the successful recapitulation of the XCGD phenotype could be demonstrated *in vitro*. Unlike PLB cells where targeted disruption of the *CYBB* gene was necessary to establish the XCGD model, the original point mutation that had been identified was successfully retained in XCGD-iPSCs generated from the patient. This translated into a complete absence in expression of gp91phox and ROS production in neutrophils differentiated from untransduced XCGD-iPSCs. To date, these are the only known defects with XCGD neutrophils as other elements of functionality such as phagocytosis are thought to be normal. In this study, it could be demonstrated that the phagocytic capacity of XCGD neutrophils remained intact and that cells are not able to generate NETs. Taken together, it may be concluded that this is a reliable model that can accurately recapitulate the disease phenotype and can be used to elucidate previously unreported pathophysiological mechanisms that may be unique to XCGD.

It was found that cellular recovery (gp91phox expression and ROS production) in neutrophils differentiated from gp91phox-transduced XCGD-iPSCs was incomplete. This is consistent with a previous report of XCGD modeling using an alpharetroviral vector design that is similar to the ones used in this study [(52)]. In that report, gp91phox-transduced XCGD $CD34^+$ cells from a patient were induced to undergo granulocyte differentiation. However, it was also found that the recovery of ROS production on a per cell basis was incomplete compared to the wild type control. For most research purposes, XCGD $CD34^+$ cells can be difficult to obtain in sufficient numbers that will allow experiments to be repeated intensely. In this study, preliminary experiments aimed at optimizing the *in vitro* neutrophil differentiation

procedure included the use of $CD34^+$ cells from a healthy individual. However, the kinetics of differentiation appears to be different in that a longer period of time is required to obtain mature neutrophils (data not shown). Considering that similar observations were made in the aforementioned study, this study focused solely upon the use of the iPSC system.

One possible explanation for the incomplete cellular recovery observed could be due to insufficient transgene expression. The strength of promoter activity could be raised to increase gp91phox expression thus the SFFV promoter was also assessed. However, cellular recovery remained far less compared with the wild-type control on a per cell basis. This may in part be attributed to promoter silencing. Future plans to include bisulphite sequencing of the promoter regions may indicate the extent of methylation that has occurred [61]. Nonetheless for most experimental purposes, the activity of the EFS promoter is considered to be strong enough to confer stable and long-term transgene expression. To account for the possible susceptibility of promoter silencing in this system, puromycin selection pressure was sustained throughout from the maintenance of transduced iPSCs to the end of the differentiation process to ensure consistent selection of gp91phox-expressing cells. Additionally it could be confirmed that in some cases, the estimated VCN was as high as 9.25 (EFS) and 14.15 (SFFV) respectively (Table 1). Still, cellular recovery remained incomplete therefore promoter silencing alone may not fully explain observations made in this study.

In this study, there were two specific findings to suggest that ectopic gp91phox expression may specifically be exerting a detrimental effect on neutrophils. In a previous study comparing global gene expression in polymorphonuclear neutrophils (PMNs), it was found that compared with healthy individuals, there was a 3.1 fold down-regulation in *CYBB* (gp91phox) expression in XCGD patients, which correlated with an opposite 2.7 fold increase in *NCF1* (p47phox) gene expression [62]. In this study, a negative correlation could be identified at the protein level between gp91phox and p47/67phox expression. Given that direction of response appears to be an opposing one, it appeared that non-physiologically regulated gp91phox expression could lead to detrimental effects. In addition, previously it had been reported that neutrophils could be induced to undergo apoptosis following sustained ER-stress [63]. In this study, we attempted to evaluate the levels of ER-stress in the developing

fraction of differentiating neutrophils. The expression of the ER stress markers GRP78, pEIF2α, pJNK and XBP-1 were determined. Relative expression was calculated by subtracting the MFI of each marker in the NGFR -ve fraction from the NGFR +ve fraction (Figure 30). It was found in the XCGD group that there was a significant increase in GRP78 expression in developing neutrophils ectopically expressing gp91phox (Figure 31a, XCGD, Ectopic gp91 vs. Control). Interestingly, the presence of ectopic gp91phox protein corresponded with a significant increase in pEIF2α expression in healthy cells (Figure 31b, Healthy, Ectopic gp91 vs. Control). No statistically significant differences could be detected for pJNK and XBP-1. NADPH oxidase-derived ROS is known to be capable of inducing ER-stress [(56)]. However, not all of the markers tested show raised expression plus the fact that there appears to be differences in response between healthy and XCGD cells ectopically expressing gp91phox. Although it cannot be concluded that induced ER-stress is the main underlying mechanisms leading to induced apoptosis, the data do suggest that these cells may have the propensity for undergoing such a fate. Therefore cell viability was determined in cells ectopically expressing gp91phox but given the wide range of physiological functions of NADPH oxidase, it is possible that perturbations in ROS production may lead to other effects.

For the ER-stress and cell apoptosis assays, it was necessary to lift puromycin selection at the start of neutrophil differentiation, which may otherwise compromise cell viability in additional to potential ectopic gp91phox involvement. At this point, all cells are transgene positive. Since gp91phox can be detected in differentiated cells but not iPSCs, ΔLNGFR (truncated NGFR) was selected as an additional selection marker to identify transgene positive cells throughout the differentiation process. 2A peptides were used for vector construction, which was previously demonstrated to be effective at ensuring efficient and robust multicistronic expression of multiple transgenes in ESCs [(64)]. However, it remains unclear in neutrophils whether all transgene-derived gp91phox becomes the stably assembled or whether any excess is subsequently degraded. This information would be necessary for establishing a threshold of tolerance in cells to non-physiological ROS production. In addition, from the results of this study, it is not possible to rule out the possibility that cell death may be caused by direct toxicity to the gp91phox protein itself. Future work may be

necessary to use a mutant form of gp91phox in which the protein is translated but ROS generating capacity remains abolished [65].

In order to offer cellular protection from non-physiological ROS production, it would be important to know the precise point during hematopoietic differentiation that ectopic gp91phox expression will begin to exert detrimental effects. In the context of this study, it can only be concluded that the impediment occurs after cells have committed to the granulocyte lineage somewhere during the transition from developing to mature neutrophils. Earlier during hematopoietic differentiation, it is known that NOX2 expression is very low in stem or progenitor hematopoietic cells but becomes much higher in mature phagocytes [30]. Theoretically primitive hematopoietic cells may express insufficient levels of additional NOX2 subunits to support the stability of overexpressed transgene-derived gp91phox. To date, it remains to be seen whether constitutive overexpression of gp91phox can compromise the functionality or engraftment potential of HSCs [24]. Nonetheless, transgene expression should be avoided in this population in order to minimize any genotoxic risks [66]. Recently a dual-regulatory strategy of gene expression combining transcriptional and posttranscriptional regulation was demonstrated. In that study, a lentiviral vector with a myeloid specific promoter and two micro RNA 126 "sponge" sequences were shown to effectively restrict gp91phox expression to the myeloid compartment with minimal leakage [67]. These sponge sequences are nucleotides complementary to micro RNA 126, which is highly expressed in hematopoietic cells up to the myeloblast/promyelocyte stage of development. They are located in tandem at the end of a vector transcript and leads to degradation of the vector transcript when the micro RNA in questions binds to it. In the context of this study, this method of lineage-restricted expression of gp91phox may eliminate some of the impediment imposed upon developing cells that can differentiate into mature neutrophils. There is also the additional benefit of sparing the HSC compartment, making it a promising approach to improve XCGD gene therapy in the future. Recently an XCGD clinical trial had been initiated using a lentiviral vector with an internal myeloid promoter. The outcomes to this trial may yet offer further insights as to whether myeloid restricted expression of gp91phox can lead to higher percentages or more sustained level of gene marking in the myeloid compartment. Alternatively, cellular protection may be offered more by directly antagonizing the effects of non-physiological ROS

production. This may be aimed at a more specific target such as using chemical agents to reduce the levels of ER-stress [68] or administer a more generalized ROS scavenger such as N-acetylcysteine (NAC) [69]. If this method of cellular protection is to be adopted then further determination of the precise cause of cell death plus timing of drug administration will be necessary.

For XCGD, alongside other monogenetic hematological disorders, gene correction in HSCs is the definitive way of restoring gene expression under physiological control. Currently there is a number of nuclease-based genome editing techniques available for this purpose. These include the use of zinc finger nucleases (ZFNs), transcription activator-like effector nucleases (TALENs), clustered regularly interspaced short palindromic repeat (CRISPR)-associated nuclease Cas9 and meganucleases [70]. The concept behind each method is similar where the idea is to introduce DNA double-stranded breaks (DSBs) at the site of mutation followed by homology-directed repair (HDR) using an exogenous template and the endogenous cellular repair machinery to mediate gene repair. Of these technologies, the CRISPR-Cas9 has emerged as the most promising given its ease of practicality in application. It utilizes RNA molecules to target specific DNA binding sequences as opposed to much larger protein complexes and there are reduced incidences of off-site targeting [71]. Compared with other methods, the CRISPR-Cas9 system can offer similar degrees of specificity whilst being considerably cheaper to synthesize thus making its application more practical. Recently gene correction using ZFNs was demonstrated in HSCs taken from an individual from SCID-X1 [72], a disease cause by a mutation in the *IL2RG* gene. Gene edited cells could reconstitute sustained functional hematopoiesis in NSG mice. However, it should be noted that similar to observations from clinical trials, corrected cells have a selective growth advantage since the *IL2RG* gene is essential for the development of lymphoid cells. Therefore the editing efficiency, as determined by the efficiency in gene transfer and homology directed DNA repair, does not need to be particularly high. However, in the case of XCGD, NADPH oxidase is not know to improve the fitness of corrected cells thus a greater level of therapeutic efficiency will be required compared with other diseases. In addition, whilst there is certainly promise in all of these genome-editing techniques, the required method of *in vitro* delivery of nuclease and repair components (electroporation and viral transduction) as well as the length of time required to complete gene correction can negatively

compromise the function of HSCs. Taken together, despite advancements in editing techniques, successful outcomes is likely to be dependent on whether correction could be achieved without compromising HSC "stemness" and by maximizing the therapeutic efficiency.

An interesting question to ask would be the extent of recovery that could be expected whether the strategy is to antagonize non-physiological ROS production or to adopt lineage restricted expression of gp91phox. Worth keeping in mind is that even if curative treatment is not yet possible by either strategy, it is known that even an improvement in 0.5% sustained gene marking could lead to a significant improvement in the quality of life of XCGD patients (personal communication with Dr. Harry Malech, Laboratory of Host Defenses, NIH, USA). In a clinical trial carried out at the NIH in the USA, stable gene marking at 0.5% was achieved in an XCGD patient who received HSGT using the MFGS-gp91phox vector with conditioning (busulfan 10 mg/kg) [(73)]. Although drug prophylaxis remains a necessity, the frequency of emergency intervention has been reduced significantly. Therefore a complete cure may not be necessary to bring meaningful benefit to the patient.

In summary, by using XCGD iPSCs as a modeling platform to assess the effects of constitutive transgene expression, an alternative prospective of this disease is offered. It is possible that cellular recovery may be raised by greatly increasing the number of provirus insertions. However, this may narrow the therapeutic window, which is a delicate balance between raising gp91phox expression and the associated genotoxic risks as the same time. There is promise in that ROS antagonists such as NAC is already in clinical use to treat a range of existing diseases including pulmonary and neurological disorders [(74)] but it remains to be seen how this may apply to XCGD. The evidence here also supports the current trend in HSGCT of lineage restricted transgene expression as this strategy may both minimize the genotoxic risk and improve neutrophil viability at the same time. It is hoped that further study using this iPSC modeling system may yet yield additional therapeutic targets the resolution of which could lead to improvements in CGD clinical outcomes.

Chapter 5. Figures and tables

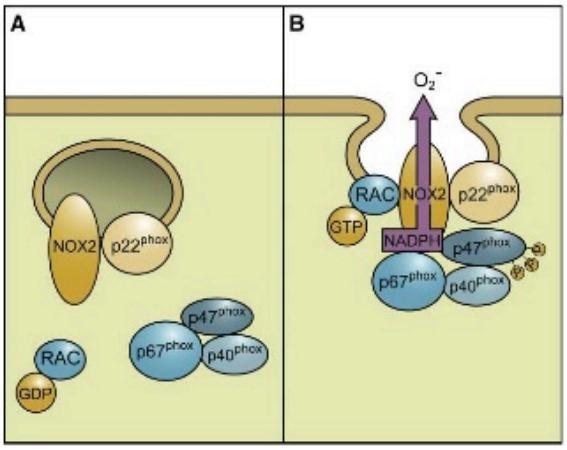

Figure 1. Assembly of NADPH oxidase.

(a) In the resting state, gp91phox (also known as NOX2) is found in a stable dimerized form with p22phox whilst the remaining components (p47phox, p67phox and p40phox) remain in the cytoplasm. (b) Upon stimulation, the cytoplasmic components translocate to the membrane and become part of the fully assembled NADPH oxidase where molecular oxygen is converted into superoxide anion. Adopted from Bedard et al [30].

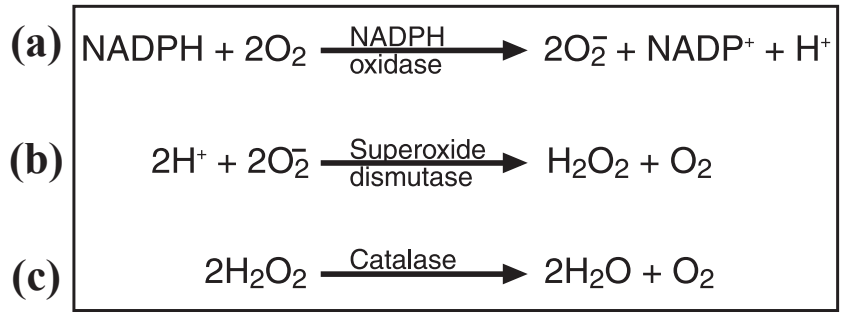

Figure 2. ROS generation from the "respiratory burst". (a) NADPH oxidase catalyzes the conversion of molecular oxygen into superoxide anion (O_2^-). (B) Rapid conversion of O_2^- into hydrogen peroxide (H_2O_2) by superoxide dismutase. (C) H_2O_2 stabilizes further into water (H_2O) and molecular oxygen (O_2). Modified from Yamazaki et al [(75)].

CGD gene	Genetic Transmission	Frequency (%)
gp91phox (CYBB)	X-linked	65
p47phox (NCF1)	Autosomal recessive	25
p67phox (NCF2)	Autosomal recessive	5
p22phox (CYBA)	Autosomal recessive	5

Table 1. CGD classification.

Subtypes of CGD based on actual diagnosed cases alongside the mode of inheritance and frequency of occurrence. Adopted from Assari [76].

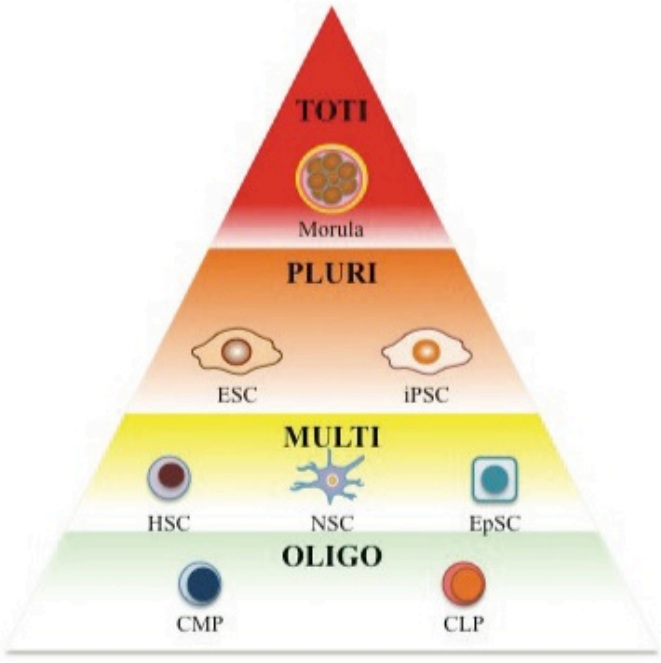

Figure 3. A hierarchical order based on cell potency.

TOTI, totipotent; PLURI, pluripotent; MULTI, multipotent; OLIGO, oligopotent; ESC, embryonic stem cell; iPSC, induced pluripotent stem cell; HSC, haematopoietic stem cell; NSC, neural stem cell; EpSC, epithelial stem cell; CMP, common myeloid progenitor; CLP, common lymphoid progenitor. Adopted from Lin et al [33].

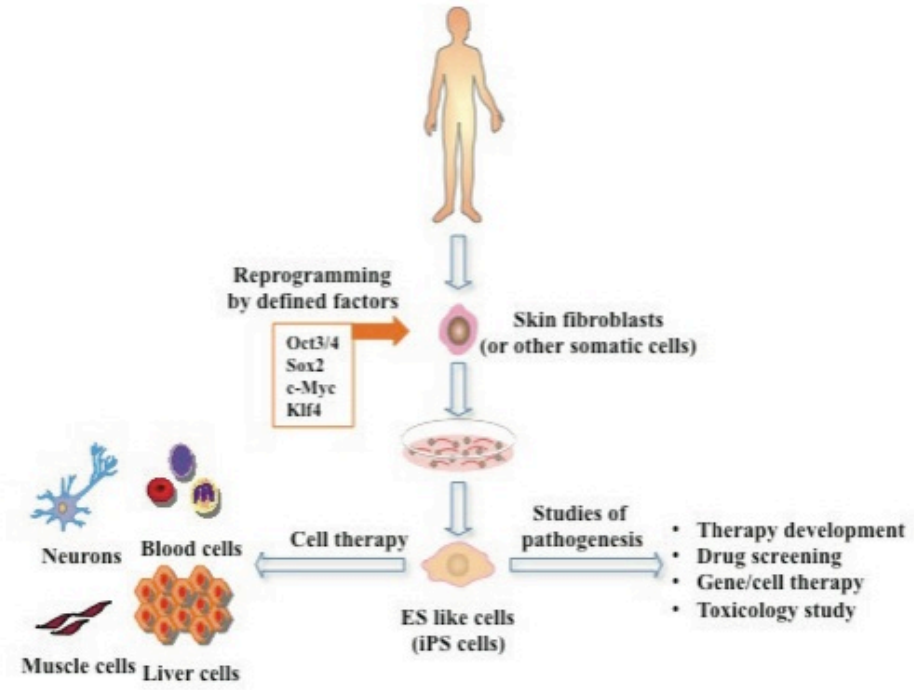

Figure 4. Generation and practical application of iPSCs.

Somatic cells from a patient may be reprogrammed to pluripotency whilst retaining a known gene mutation. iPSCs may be differentiated along numerous different lineages and have applications in transplantation therapy or disease modeling. Adopted from Lin et al [33].

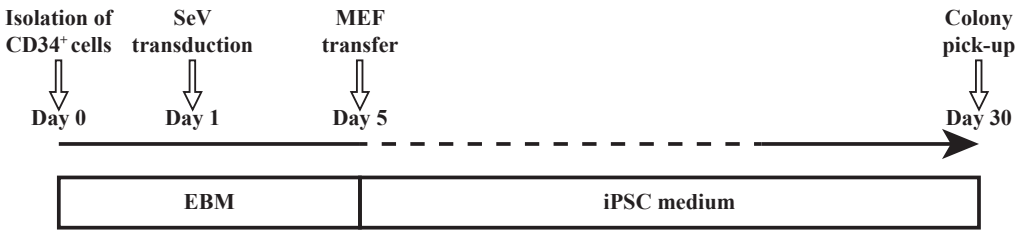

Figure 5. Reprogramming XCGD PB CD34+ cells into iPSCs.

Schematic overview of the reprogramming process using a Sendai virus (SeV) vector carrying the four Yamanaka factors to transduce peripheral blood (PB) $CD34^+$ cells. XCGD iPSC (#8) was subjected to detailed characterization and used for subsequent experiments. Embryoid body medium (EBM).

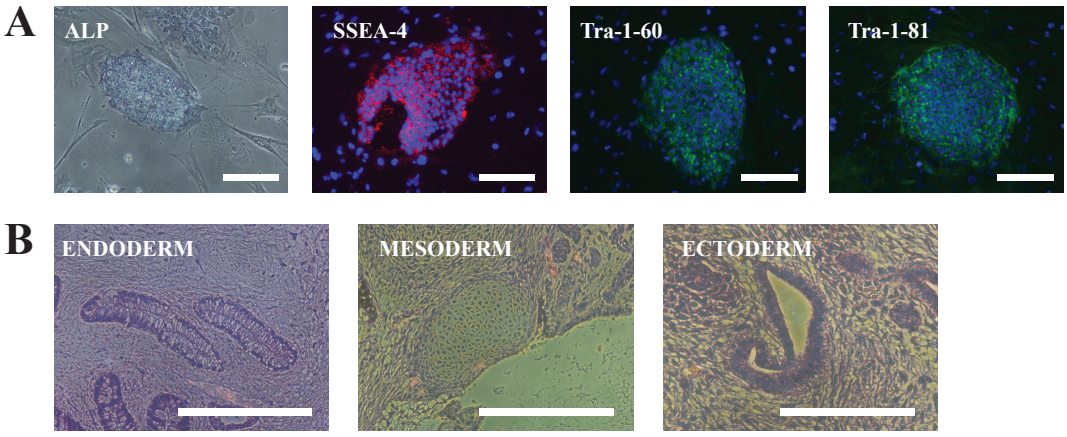

Figure 6. Characteristic features of pluripotency.

(a) XCGD iPSCs stained positive for ALP, SSEA-4, Tra-1-60 and Tra-1-81. (b) XCGD iPSCs could form teratomas consisting of tissue derived from the three germ layers endoderm, mesoderm and ectoderm. Scale bars = 200 μm

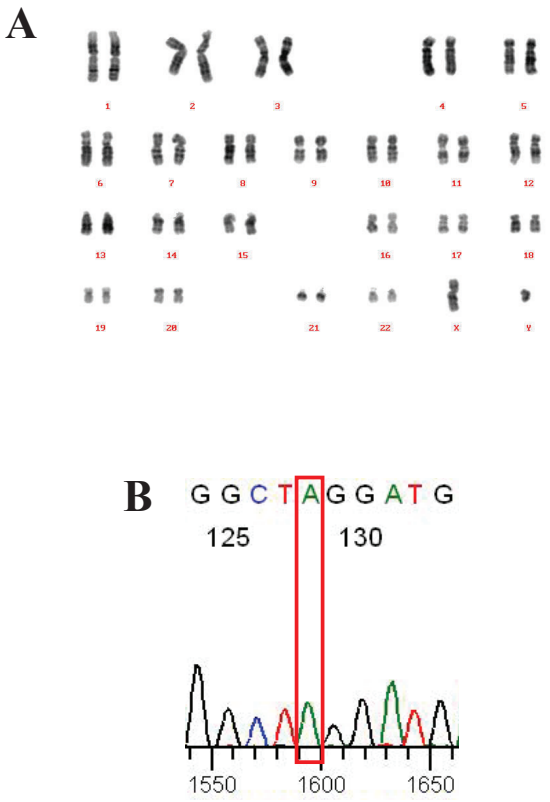

Figure 7. Karyotyping of XCGD iPSCs and retention of the *CYBB* mutation.

(a) A normal karyotype was exhibited. (b) Confirmation of the point mutation *CYBB*: c.1448G>A (p.Trp483X).

Gene	Primer Orientation	Sequence
OCT3/4	F	5'-ATTCAGCCAAACGACCATC-3'
	R	5'-GGAAAGGGACCGAGGAGTA-3'
SOX2	F	5'-CAGCGCATGGACAGTTAC-3'
	R	5'-GGAGTGGGAGGAAGAGGT-3'
c-MYC	F	5'-AGTTTCATCTGCGACCCG-3'
	R	5'-CCTCATCTTCTTGTTCCTCCT-3'
KLF4	F	5'-GCGGGAAGGGAGAAGACA-3'
	R	5'-CCGGATCGGATAGGTGAA-3'
NANOG	F	5'-CAGCCCTGATTCTTCCACCAGTCCC-3'
	R	5'-TGGAAGGTTCCCAGTCGGGTTCACC-3'
GAPDH	F	5'-AACAGCCTCAAGATCATCAGC-3'
	R	5'-TTGGCAGGTTTTTCTAGACGG-3'

Table 2. Primer sequences used for detecting pluripotency genes

Shown are the precise sequences for both the forward (F) and reverse (R) primers used to detect pluripotency genes by RT-PCR.

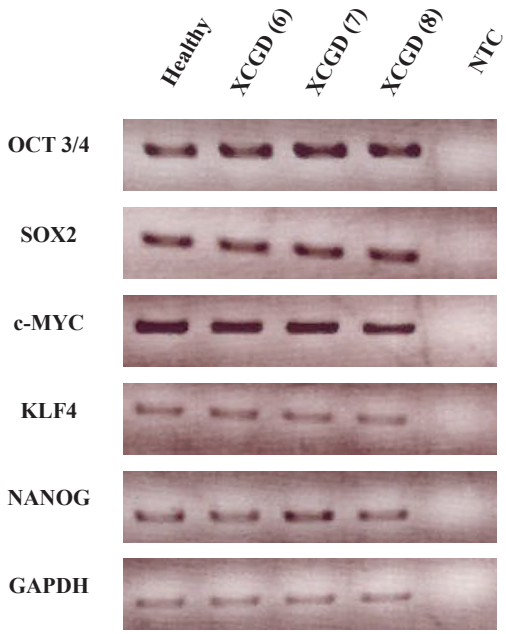

Figure 8. Analysis of pluripotency genes by RT-PCR.

Three XCGD iPSC clones (#6-8) were checked for the expression of pluripotency genes. Healthy iPSCs were used as the positive control. GAPDH served as the internal control. Non-template control (NTC).

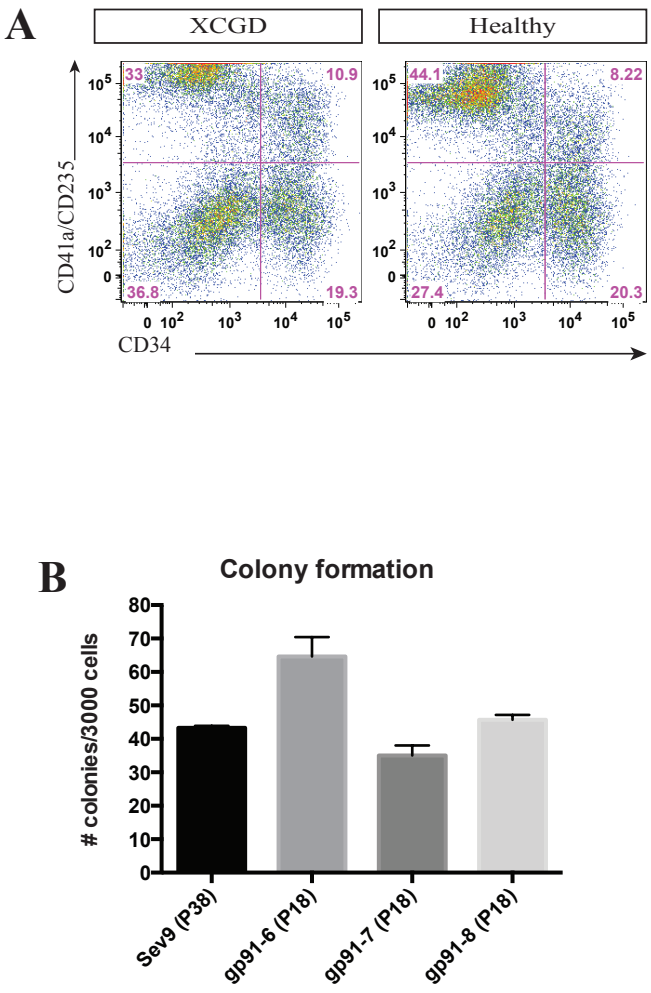

Figure 9. Colony forming potential of HPCs.

(a) Following exclusion of committed CD41a and CD235 (Lineage) positive cells, $CD34^{+}Lin^{-}$ cells were sorted from Day14 HPCs and subjected to the hematopoietic colony forming assay. (b) After 12 days of culture, the total numbers of colonies per 3000 input cells are counted.

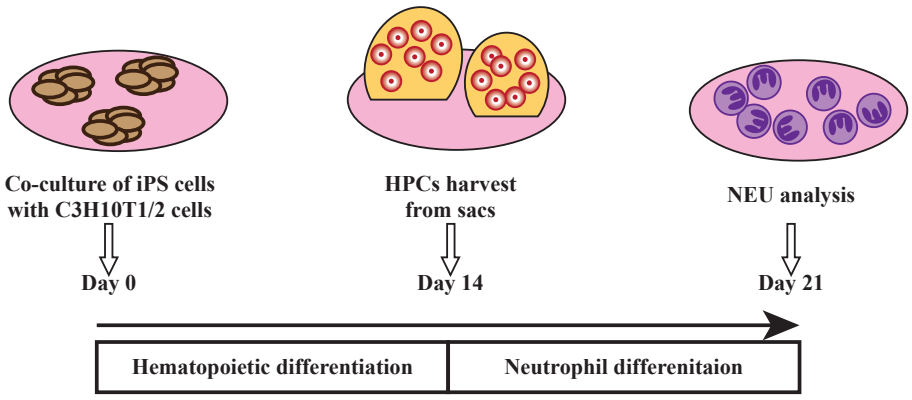

Figure 10. Schematic overview of neutrophil differentiation from iPSCs.

Detached iPSCs were co-cultured on a layer of C3H10T1/2 cells and induced to undergo hematopoietic differentiation. 14 days later, HPCs could be harvested from sac-like structures and then further induced to undergo neutrophil differentiation. After an additional 5 to 7 days, differentiated cells may be subjected to further analyses.

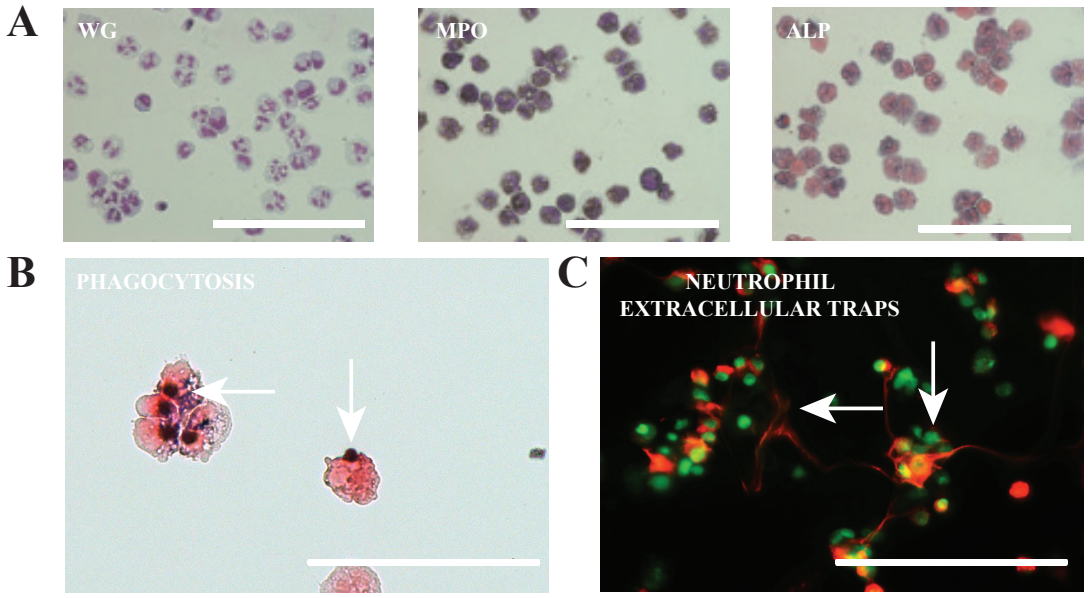

Figure 11. Morphology and functional assessment of differentiated neutrophils. (a) Histological appearance of differentiated neutrophils. Wright Giemsa (WG) staining, myeloperoxidase (MPO) (black dots) and alkaline phosphatase (ALP) (purple dots). (b) NBT-coated yeast were added to a suspension of differentiated cells for 1 hour at 37°C and then stained with 1% safranin-O. Phagocytosed yeast is black in color due to the reduction of NBT to formazan by ROS (white arrows). (c) Differentiated cells were seeded onto Poly-L-Lysine coated cover slips and stimulated with PMA to induce the formation of neutrophil extracellular traps (white arrows). After permeabilization and fixation, cells were stained for SYTO 13 (green) and MPO (red).

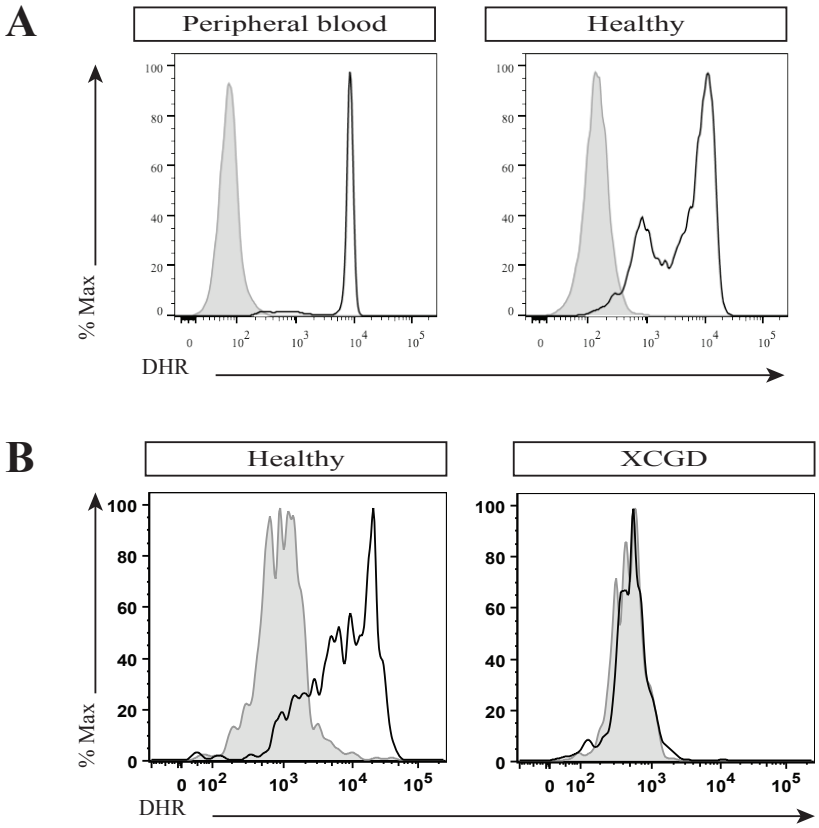

Figure 12. ROS production in neutrophils and recapitulation of the XCGD phenotype.

To assess functionality, neutrophils were stimulated with PMA and then assessed for ROS production by the DHR assay. (a) Following stimulation, neutrophils differentiated from healthy iPSCs showed similar intensity in ROS production compared with PB neutrophils. (b) Recapitulation of the XCGD phenotype is shown by demonstrating that neutrophils differentiated XCGD iPSCs showed no oxidase activity. Non-stimulated (grey) and stimulated cells (black line).

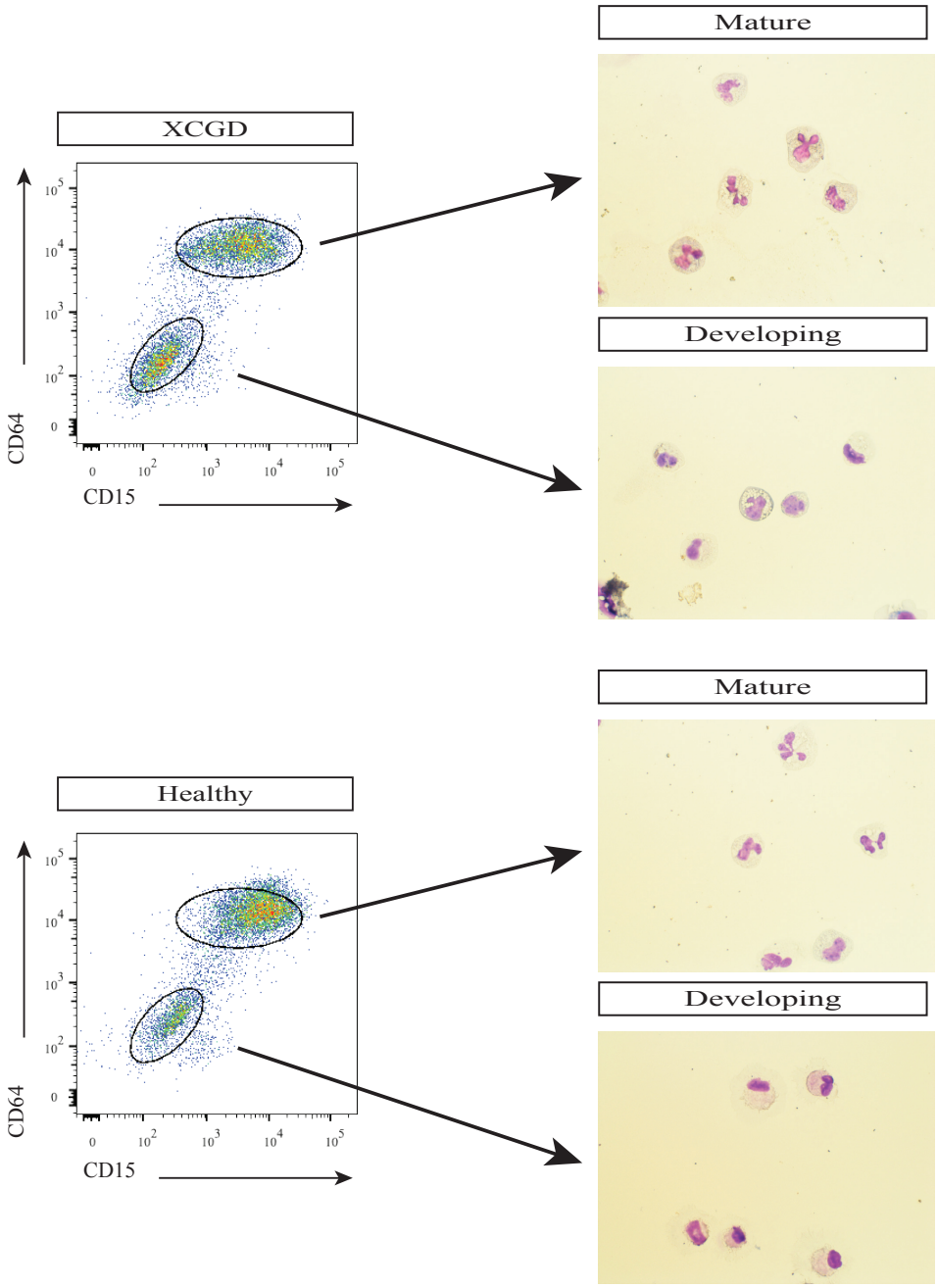

Figure 13. Immunophenotype and morphology of differentiating neutrophils. Within the same differentiation culture, both developing ($CD64^{low}CD15^{low}$) and mature ($CD64^{High}CD15^{High}$) neutrophils could be identified regardless of differentiation from an XCGD or healthy genetic background. Following cell sorting, it can be seen that in the mature fraction, most of the cells are either band or segmented neutrophils. In the developing fraction, cells have the appearance of either myelobalsts or myelocytes.

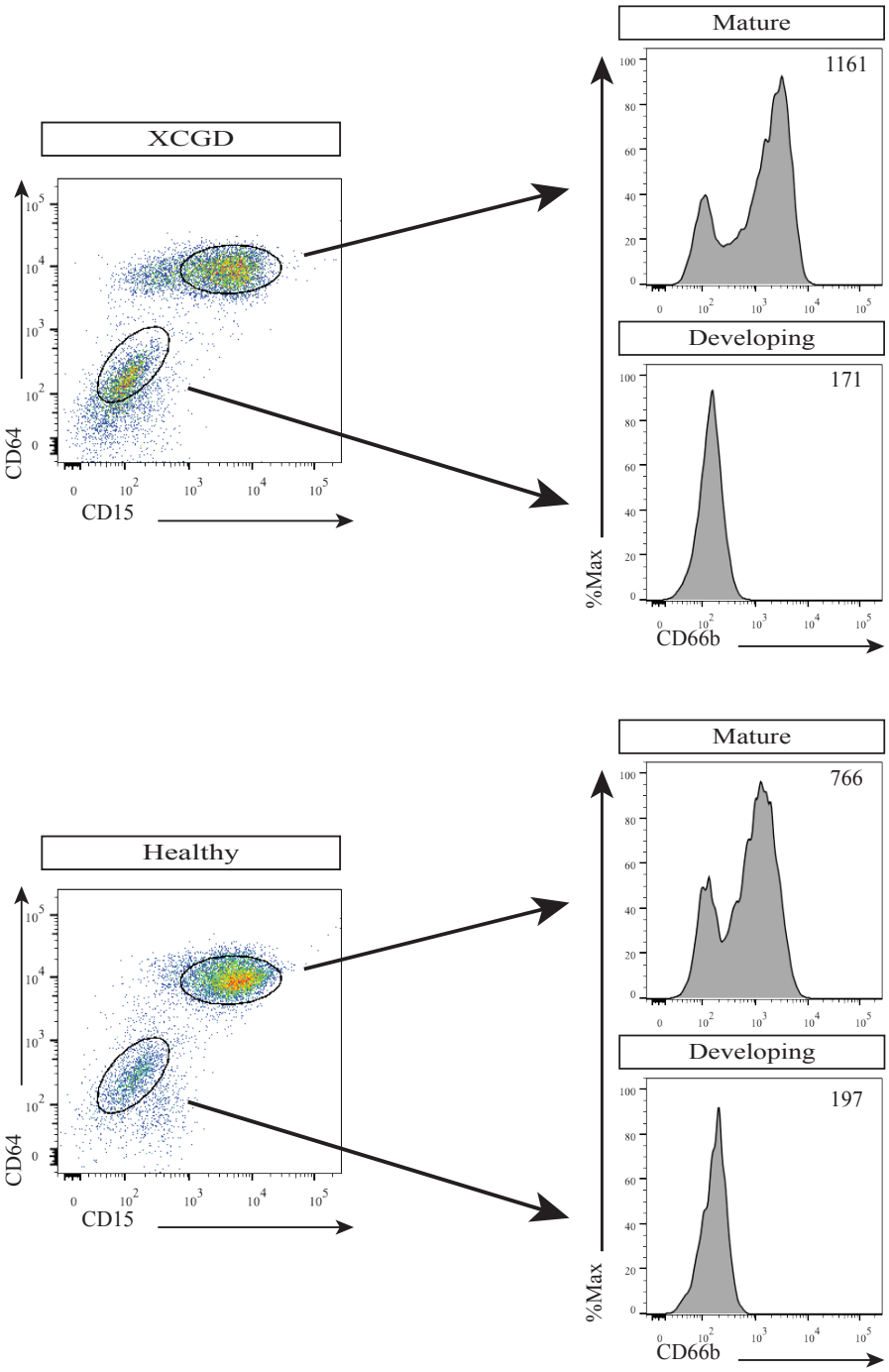

Figure 14. Mature neutrophils express greater levels of CD66b.

CD66b is a surface adhesion molecule the expression of which can be used to characterize mature neutrophils. To further support the use of CD64 and CD15 expression to define neutrophil maturation status, within the same staining sample, differences in CD66b expression (grey histogram) were determined in developing and mature neutrophils differentiated from either an XCGD or healthy genetic background. Numbers indicate the mean fluorescence intensity (MFI).

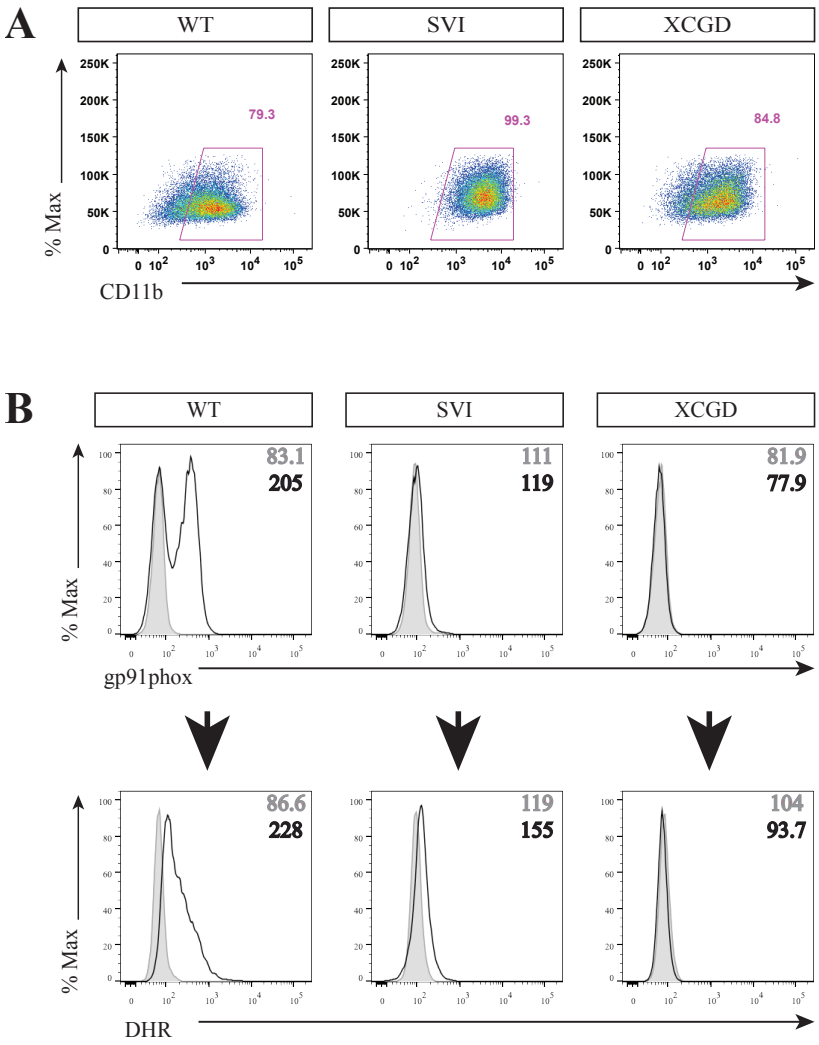

Figure 15. CGD modeling using PLB cells.

(a) PLB 985 cells can be induced to undergo granulocytic differentiation as indicated by the expression of CD11b. (b) Following differentiation, only the WT cells (PLB-WT) showed significant expression of gp91phox. Similarly only WT cells demonstrated significant ROS production. Numbers indicate the MFI.

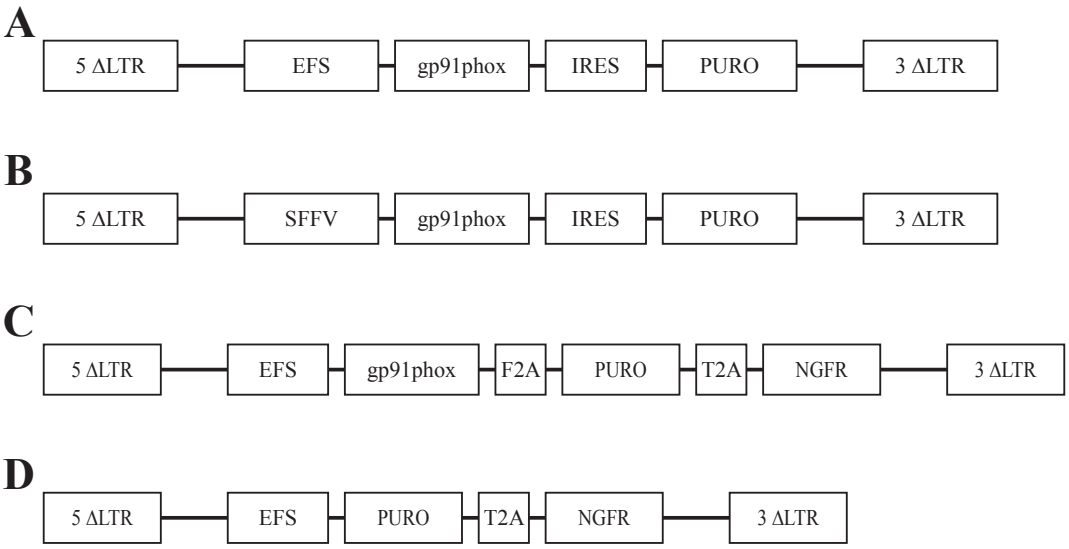

Figure 16. Schema of alpharetroviral proviruses.

The same vector backbone was used regardless of the modifications made in design:

(a) pAlpha.SIN.SFFV.gp91s.IRES.PURO.oPRE

(b) pAlpha.SIN.SFFV.gp91s.IRES.PURO.oPRE

(c) pAlpha.SIN.EFS.gp91s.F2A.PURO.T2A.NGFR.oPRE

(d) pAlpha.SIN.EFS.PURO.T2A.NGFR.oPRE

(This section cannot be made public on the Internet for 5 years from the date of doctoral degree conferral because it is currently under review and has yet to be accepted for publication.)

Figure 17. Primer design for detecting codon optimized CYBB.
Bidirectional arrows indicate differences in base sequences between codon optimized (white letters) and genomic (grey letters) *CYBB*.

(This section cannot be made public on the Internet for 5 years from the date of doctoral degree conferral because it is currently under review and has yet to be accepted for publication.)

Figure 18. Target specificity.

Amplification curves for the detection of CO *CYBB* and puromycin (pink) as well as genomic *CYBB*. The transfer plasmid pAlpha.SIN.EFS.gp91s.F2A.PURO.T2A.ΔLNGFR.oPRE was diluted to 10 and 100 times respectively. As a control, plasmid DNA containing non-codon-optimized *CYBB* cDNA but no *PURO* sequence was used as template. Horizontal pink line represents the C_t (threshold cycle). Relative fluorescence units (RFU). No template control (NTC).

(This section cannot be made public on the Internet for 5 years from the date of doctoral degree conferral because it is currently under review and has yet to be accepted for publication.)

Table 3. Cycle threshold values for the detection of codon optimized CYBB and puromycin.

Summary of CO *CYBB* and puromycin detection alongside the respective C_t (threshold cycle) values. Not applicable (N/A) indicates no detection. No template control (NTC).

(This section cannot be made public on the Internet for 5 years from the date of doctoral degree conferral because it is currently under review and has yet to be accepted for publication.)

Figure 19. VCN estimation in PLB cells.

To estimate the average VCN, the concentration (copies/ul) of the target transgene (dark blue) and the *RPP30* (green) reference gene needs to be determined in a given sample. This may be done either in singleplex (light blue, single primer probe) or in multiplex (pink, both probes). gDNA were extracted from three different types of PLB cells containing the following provirus insertions; SC91 (single copy pAlpha.SIN.EFS.oPRE), E91P (pAlpha.SIN.EFS.IRES.PURO.oPRE) and S91P (pAlpha.SIN.SFFV.IRES.PURO.oPRE). No template control (NTC).

(This section cannot be made public on the Internet for 5 years from the date of doctoral degree conferral because it is currently under review and has yet to be accepted for publication.)

Table 4. VCN estimation in PLB cells.

To estimate the VCN in each sample, the relative concentration of the target gene (x2) is divided by the relative concentration of the reference RPP30 gene. Where applicable this may be calculated by referring to the concentration of either CO *CYBB* or puromycin.

(This section cannot be made public on the Internet for 5 years from the date of doctoral degree conferral because it is currently under review and has yet to be accepted for publication.)

Table 5. VCN estimation in transduced iPSCs.

The concentration of CO *CYBB*/puromycin and RPP were measured within each sample in multiplex reactions. The average VCN were for either transduced XCGD or healthy iPSCs were then calculated. Multiplicity of infection (MOI).

(This section cannot be made public on the Internet for 5 years from the date of doctoral degree conferral because it is currently under review and has yet to be accepted for publication.)

Figure 20. RPP30 concentration remains constant despite sample dilution with non-codon optimized *CYBB*-containing gDNA.

Sample gDNA that does not contain CO *CYBB* was used as the diluent such that the number of CO *CYBB*-containing droplets (blue dots) is reduced whilst the concentration of *RPP30* positive droplets (green dots) remains constant. Pink line indicates the threshold value for assigning droplets as being positive or negative.

(This section cannot be made public on the Internet for 5 years from the date of doctoral degree conferral because it is currently under review and has yet to be accepted for publication.)

Figure 21. Assay sensitivity following sample dilution with non-codon optimized *CYBB*-containing gDNA.

To estimate the level of sensitivity of the ddPCR method, the E91PN10 sample was diluted using gDNA extracted from transduced XCGD iPSCs that do not contain codon optimized *CYBB*. Indicated are the concentrations of codon optimized *CYBB* (dark blue) and *RPP30* (green). No template control (NTC).

(This section cannot be made public on the Internet for 5 years from the date of doctoral degree conferral because it is currently under review and has yet to be accepted for publication.)

Table 6. Estimated VCN in diluted samples.

The E91PN10 sample has an estimated VCN of approximately 4 when undiluted. CO *CYBB* non-containing gDNA was used to dilute samples in order to keep the concentration of the reference *RPP30* gene relatively constant whilst reducing the concentration of codon optimized *CYBB*.

(This section cannot be made public on the Internet for 5 years from the date of doctoral degree conferral because it is currently under review and has yet to be accepted for publication.)

Figure 22. Concomitant reduction in the concentration of codon optimized CYBB and RPP30 following dilution with water.

By sample dilution with water, both the number of CO *CYBB* (blue dots) and *RPP30* (green dots) positive droplets is reduced. Pink line indicates the threshold value for assigning droplets as being positive or negative.

(This section cannot be made public on the Internet for 5 years from the date of doctoral degree conferral because it is currently under review and has yet to be accepted for publication.)

Figure 23. Determination of assay variability.

To determine the assay variability with reducing amounts of template, samples were diluted with water to the stated mass of template gDNA. With this method both the concentration of the target and *RPP30* gene is reduced. gDNA was extracted from two lines of transduced XCGD-iPSCs with known estimate VCNs of 1.1 (91PN1) and 6.8 (S91PN1) respectively. No template control (NTC). Bars represent total error at 95% confidence interval.

(This section cannot be made public on the Internet for 5 years from the date of doctoral degree conferral because it is currently under review and has yet to be accepted for publication.)

Figure 24. Pre-digestion by restriction enzymes reduces assay variability.
The S91PN1 sample was pre-digested with the restriction enzymes Not I and Bgl II. This separates tandem transgene copies and ensures single partitioning into individual droplets. The viscosity of the sample is also reduced, which would improve template accessibility to PCR amplification. Bars represent total error at 95% confidence interval.

(This section cannot be made public on the Internet for 5 years from the date of doctoral degree conferral because it is currently under review and has yet to be accepted for publication.)

Table 7. Estimation of VCN in iPSCs.

Summary of the average VCN estimate in transduced iPSCs used for neutrophil differentiation experiments. Also shown are the exact provirus insertion, genetic background of iPSCs and the MOI.

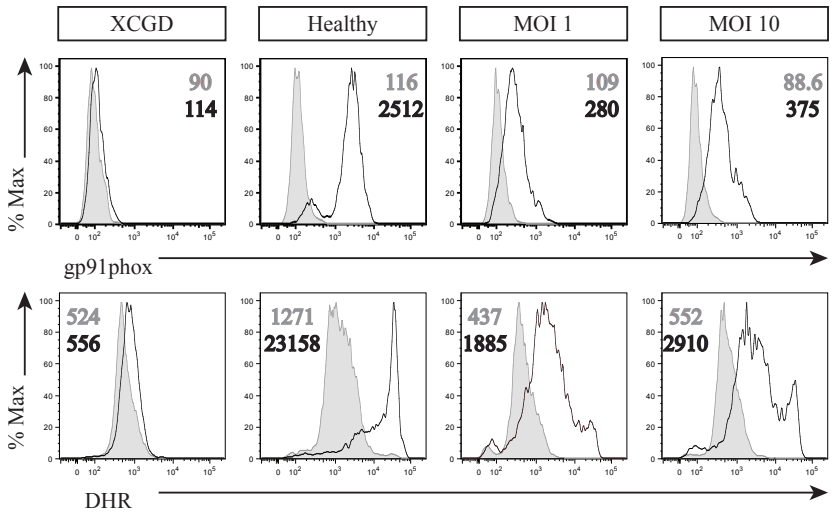

Figure 25. Cellular recovery in gp91phox expression and ROS production.

Transduced XCGD-iPSCs (MOI 1 and 10) were differentiated into neutrophils and assessed for gp91phox expression (top row) where cells were stained with the isotype control (grey) or anti-gp91phox antibody (black line). Differentiated neutrophils were also assessed for ROS production (bottom row) through the DHR assay. Non-stimulated (grey) and stimulated cells with PMA (black line). Control cells were those differentiated from untransduced XGCD or Healthy iPSCs. All numbers indicate the mean fluorescence intensity (MFI).

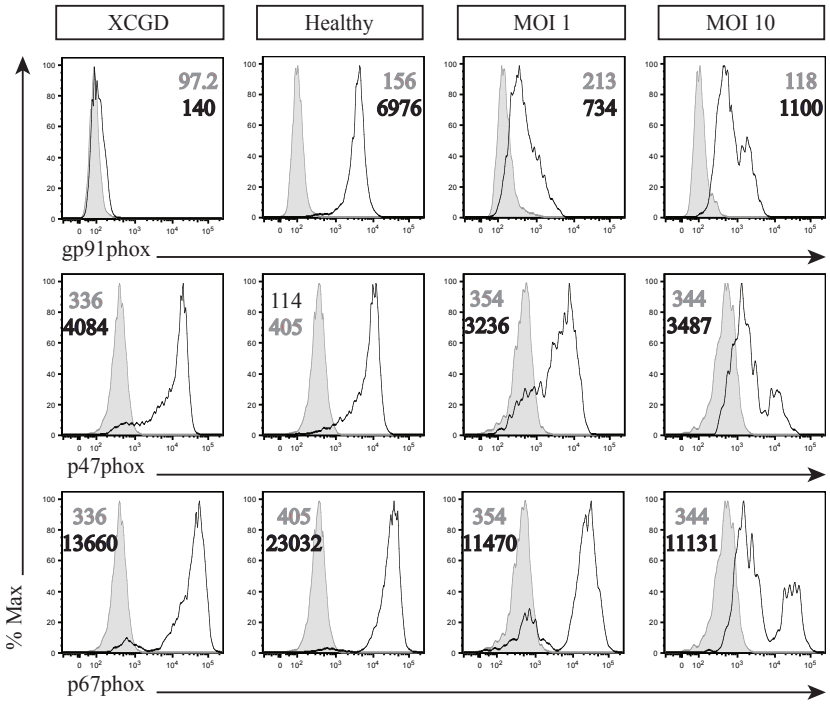

Figure 26. Correlation of gp91phox with p47/p67phox expression.

The expression of gp91phox (top row) in differentiated neutrophils was correlated with p47phox (middle row) and p67phox (bottom row) expression. Isotype control (grey) and protein expression (black lines). All numbers indicate the mean fluorescence intensity (MFI).

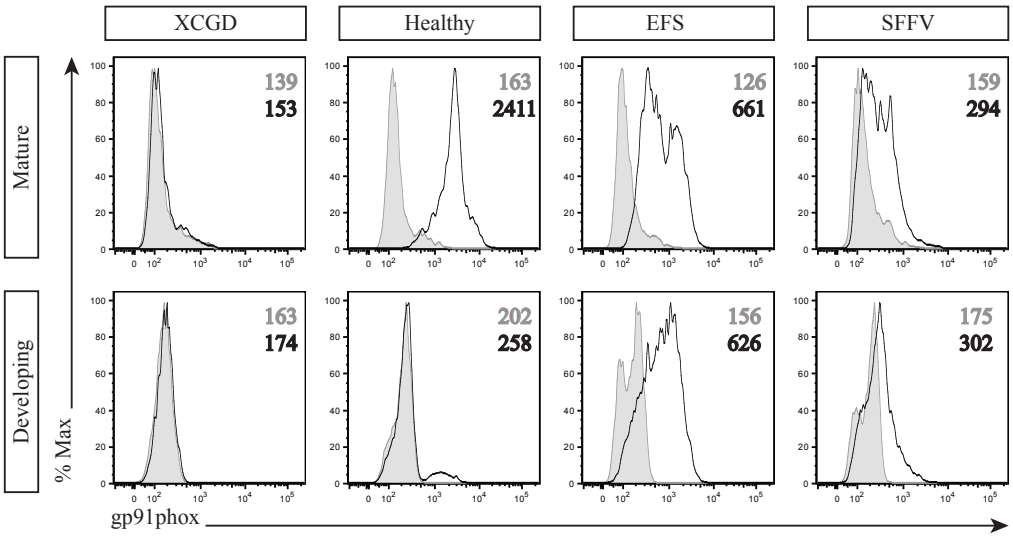

Figure 27. Ectopic expression of gp91phox in developing neutrophils.

The expression of gp91phox was assessed in mature (top row) and developing (bottom row) neutrophils. EFS and SFFV represents the type of promoters used to drive gp91phox expression. Control cells were those differentiated from untransduced healthy or XGCD iPSCs. Grey indicates the isotype control and black line indicates gp91phox expression. All numbers indicate the MFI.

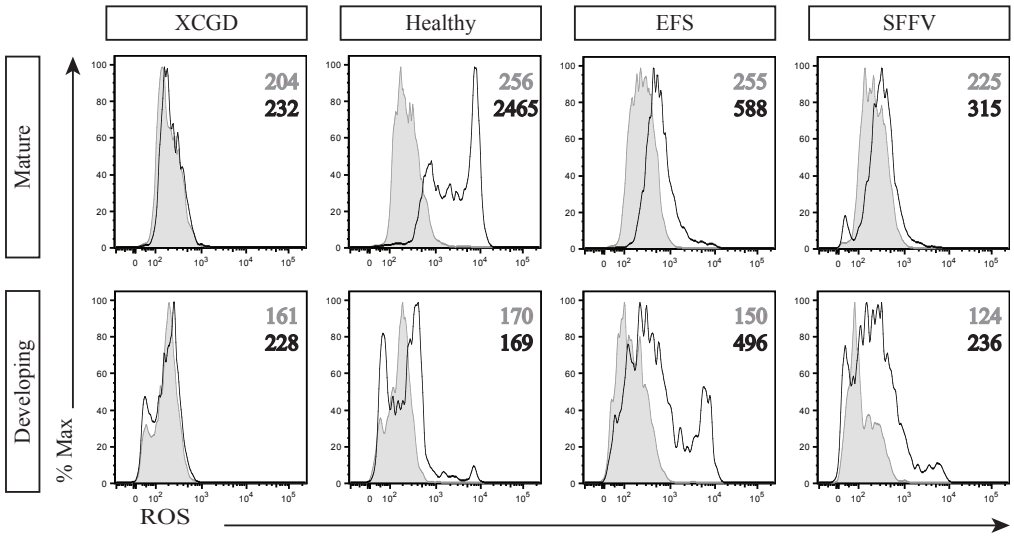

Figure 28. Non-physiological production of ROS in developing eutrophils.

Generation of ROS in mature (top row) and developing (bottom row) neutrophils. EFS and SFFV represents the type of promoters used to drive gp91phox expression. Control cells were those differentiated from untransduced healthy or XGCD iPSCs. Grey indicates no stimulation and black line indicates stimulation with PMA. All numbers indicate the MFI.

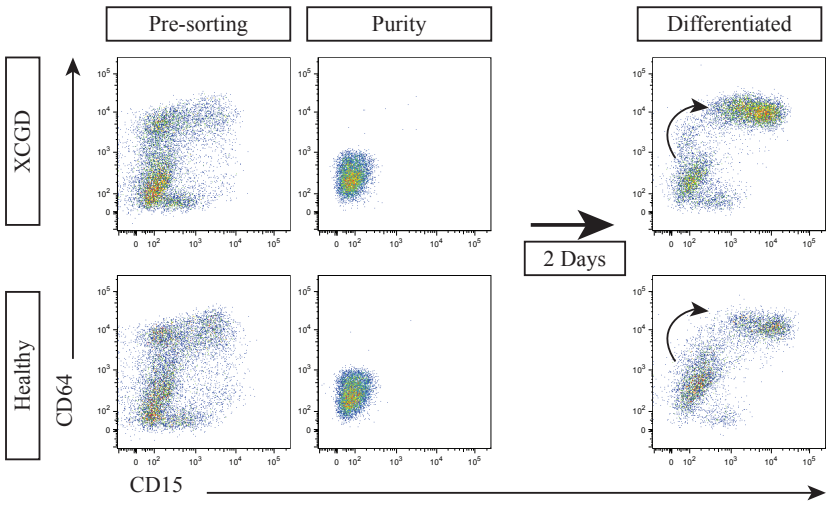

Figure 29. Hierarchical transition by differentiating neutrophils.

After 3 days of differentiation, a combination of both developing ($CD64^{dull}CD15^{dull}$) and mature ($CD64^{high}CD15^{high}$) neutrophils could be seen in the culture at this point (1st column; Pre-sorting). The developing fraction was sorted by FACS and the purity of this sorted fraction was checked (2nd column; Purity). After two further days of differentiation, the appearance of mature cells that originated from the sorted developing fraction could be identified (3rd column; Differentiated).

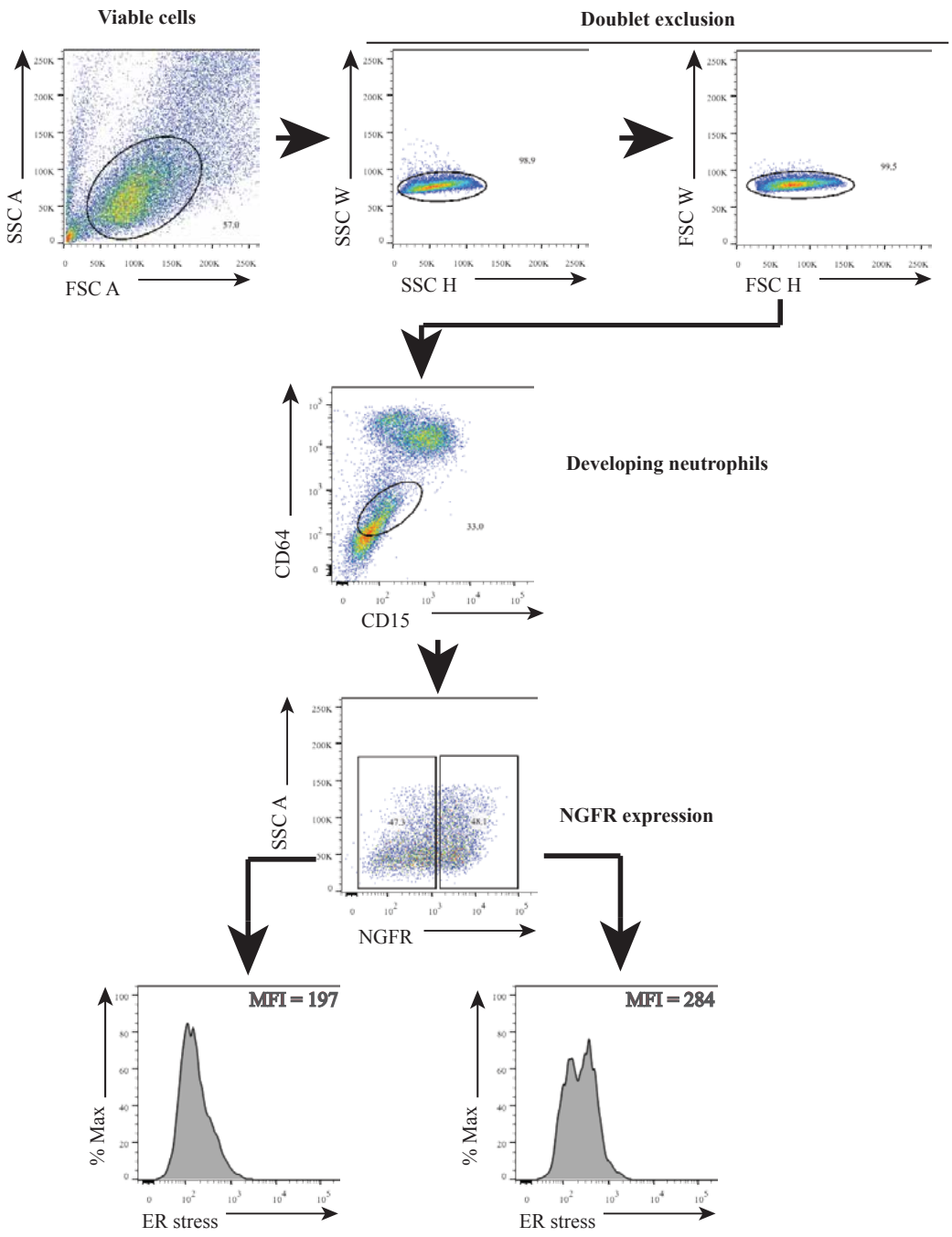

Figure 30. Representative FACS gating strategy for comparing ER stress between NGFR +ve and -ve developing neutrophils.

Firstly doublets are excluded from viable cells and then developing neutrophils ($CD64^{dull}CD15^{dull}$) are gated. The mean fluorescence intensity (MFI) of ER stress marker expression in the NGFR -ve fraction is then subtracted from the +ve fraction.

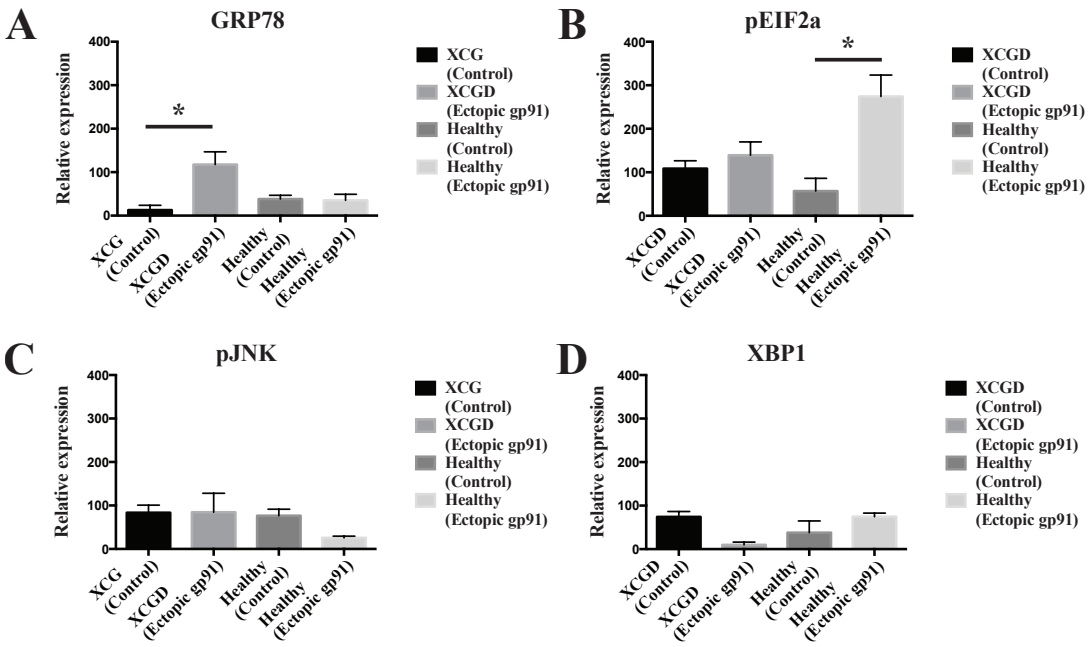

Figure 31. Expression of ER stress markers in developing neutrophils.

XCGD or healthy iPSCs were transduced with either the gp91phox-containing vector or the control vector with no gp91phox. The relative expression of each ER-stress marker in developing neutrophils was determined. Depicted are mean values + SD (n = 3, representative of 3 independent experiments). *, $p < .05$. In the XCGD group, (a) GRP78 was expressed in statistically significant levels. In the healthy group, (b) pEIF2α was found to show statistically significant raised expression. No significant expression was detected for (c) pJNK or (d) XBP-1. Neutrophils differentiated from untransduced XCGD or healthy iPSCs served as the controls.

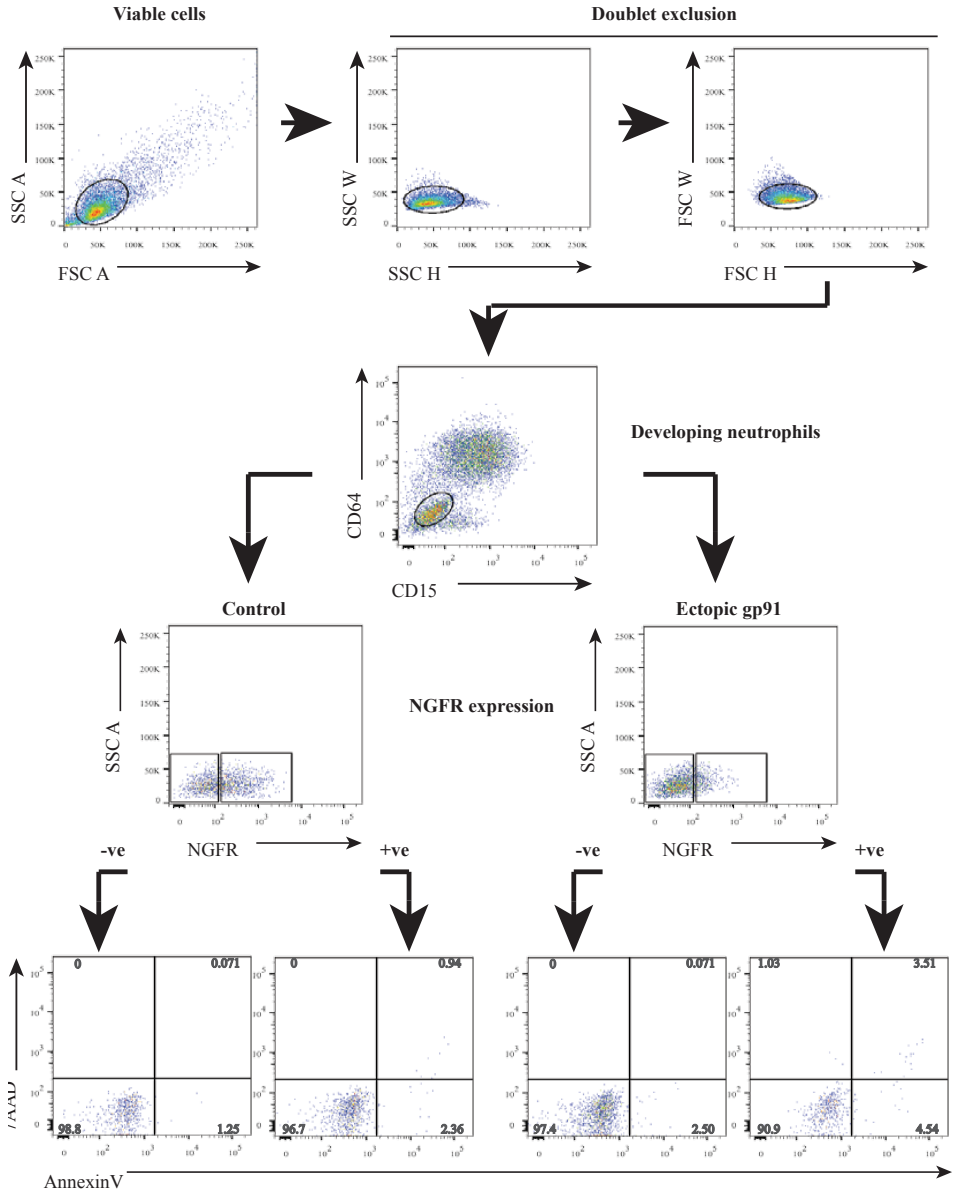

Figure 32. Representative FACS gating strategy for comparing cell viability between NGFR +ve and -ve developing neutrophils.

For all experimental samples, doublets are excluded from viable cells followed by the gating of developing neutrophils ($CD64^{dull}CD15^{dull}$). This is the representative gating strategy up to this point only for all samples. Thereafter, cell viability was determined within the NGFR –ve and +ve fractions of neutrophils differentiated from transduced with control or gp91phox-containing vector transduced XCGD iPSCs. The percentage cell death was calculated by combining the total percentage of 7-AAD-ve only, and 7-AAD/AnnexinV double positive cells.

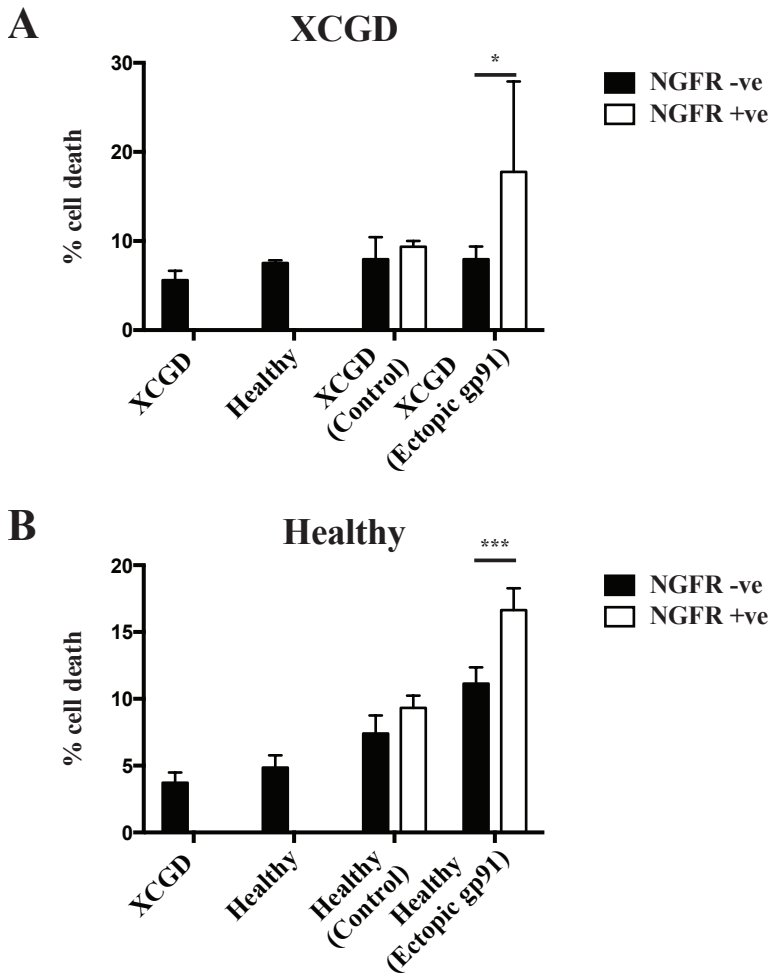

Figure 33. Developing neutrophils ectopically expressing gp91phox show reduced viability.

The 7-AAD/Annexin-V cell death/apoptosis assay was carried out to determine the viability of neutrophils in the developing fraction. NGFR expression indicates gp91phox-transgene expression in cells differentiated from iPSCs transduced with the gp91phox-containing vector. Depicted are mean values + SD (n = 3, representative of 3 independent experiments). *, $p < .05$; ***, $p < .001$. Statistically significant levels of cell death were detected in cells ectopically expressing gp91phox regardless of the genetic background. Control cells were those differentiated from untransduced healthy or XGCD-iPSCs.

References

1. Bridges RA, Berendes H, Good RA. A fatal granulomatous disease of childhood; the clinical, pathological, and laboratory features of a new syndrome. AMA J Dis Child. 1959;97(4):387-408.
2. Landing BH, Shirkey HS. A syndrome of recurrent infection and infiltration of viscera by pigmented lipid histiocytes. Pediatrics. 1957;20(3):431-8.
3. Holmes B, Quie PG, Windhorst DB, Good RA. Fatal granulomatous disease of childhood. An inborn abnormality of phagocytic function. Lancet. 1966;1(7449):1225-8.
4. Baehner RL, Nathan DG. Leukocyte oxidase: defective activity in chronic granulomatous disease. Science. 1967;155(3764):835-6.
5. van den Berg JM, van Koppen E, Ahlin A, Belohradsky BH, Bernatowska E, Corbeel L, et al. Chronic granulomatous disease: the European experience. PLoS One. 2009;4(4):e5234.
6. Ochs HD, Igo RP. The NBT slide test: a simple screening method for detecting chronic granulomatous disease and female carriers. The Journal of pediatrics. 1973;83(1):77-82.
7. Vowells SJ, Sekhsaria S, Malech HL, Shalit M, Fleisher TA. Flow cytometric analysis of the granulocyte respiratory burst: a comparison study of fluorescent probes. Journal of immunological methods. 1995;178(1):89-97.
8. Johnston RB, Jr., McMurry JS. Chronic familial granulomatosis. Report of five cases and review of the literature. Am J Dis Child. 1967;114(4):370-8.
9. Lapouge K, Smith SJ, Groemping Y, Rittinger K. Architecture of the p40-p47-p67phox complex in the resting state of the NADPH oxidase. A central role for p67phox. J Biol Chem. 2002;277(12):10121-8.
10. Borregaard N. Neutrophils, from marrow to microbes. Immunity. 2010;33(5):657-70.
11. Dinauer MC. Disorders of neutrophil function: an overview. Methods Mol Biol. 2007;412:489-504.
12. Logters T, Margraf S, Altrichter J, Cinatl J, Mitzner S, Windolf J, et al. The clinical value of neutrophil extracellular traps. Medical microbiology and immunology. 2009;198(4):211-9.

13. Jurkowska M, Kurenko-Deptuch M, Bal J, Roos D. The search for a genetic defect in Polish patients with chronic granulomatous disease. Arch Immunol Ther Exp (Warsz). 2004;52(6):441-6.

14. Battersby AC, Cale AM, Goldblatt D, Gennery AR. Clinical manifestations of disease in X-linked carriers of chronic granulomatous disease. Journal of clinical immunology. 2013;33(8):1276-84.

15. Heyworth PG, Cross AR, Curnutte JT. Chronic granulomatous disease. Current opinion in immunology. 2003;15(5):578-84.

16. Okura Y, Yamada M, Kuribayashi F, Kobayashi I, Ariga T. Monocyte/macrophage-Specific NADPH Oxidase Contributes to Antimicrobial Host Defense in X-CGD. Journal of clinical immunology. 2015;35(2):158-67.

17. Gallin JI, Alling DW, Malech HL, Wesley R, Koziol D, Marciano B, et al. Itraconazole to prevent fungal infections in chronic granulomatous disease. N Engl J Med. 2003;348(24):2416-22.

18. A controlled trial of interferon gamma to prevent infection in chronic granulomatous disease. The International Chronic Granulomatous Disease Cooperative Study Group. N Engl J Med. 1991;324(8):509-16.

19. Copelan EA. Hematopoietic stem-cell transplantation. N Engl J Med. 2006;354(17):1813-26.

20. Maetzig T, Galla M, Baum C, Schambach A. Gammaretroviral vectors: biology, technology and application. Viruses. 2011;3(6):677-713.

21. Candotti F, Shaw KL, Muul L, Carbonaro D, Sokolic R, Choi C, et al. Gene therapy for adenosine deaminase-deficient severe combined immune deficiency: clinical comparison of retroviral vectors and treatment plans. Blood. 2012;120(18):3635-46.

22. Cavazzana-Calvo M, Hacein-Bey S, de Saint Basile G, Gross F, Yvon E, Nusbaum P, et al. Gene therapy of human severe combined immunodeficiency (SCID)-X1 disease. Science. 2000;288(5466):669-72.

23. Scaramuzza S, Biasco L, Ripamonti A, Castiello MC, Loperfido M, Draghici E, et al. Preclinical safety and efficacy of human CD34(+) cells transduced with lentiviral vector for the treatment of Wiskott-Aldrich syndrome. Mol Ther. 2013;21(1):175-84.

24. Grez M, Reichenbach J, Schwable J, Seger R, Dinauer MC, Thrasher AJ. Gene therapy of chronic granulomatous disease: the engraftment dilemma. Mol Ther. 2011;19(1):28-35.

25. Malech HL, Choi U, Brenner S. Progress toward effective gene therapy for chronic granulomatous disease. Japanese journal of infectious diseases. 2004;57(5):S27-8.

26. Bianchi M, Hakkim A, Brinkmann V, Siler U, Seger RA, Zychlinsky A, et al. Restoration of NET formation by gene therapy in CGD controls aspergillosis. Blood. 2009;114(13):2619-22.

27. Stein S, Ott MG, Schultze-Strasser S, Jauch A, Burwinkel B, Kinner A, et al. Genomic instability and myelodysplasia with monosomy 7 consequent to EVI1 activation after gene therapy for chronic granulomatous disease. Nature medicine. 2010;16(2):198-204.

28. Chen C, Liu Y, Liu R, Ikenoue T, Guan KL, Liu Y, et al. TSC-mTOR maintains quiescence and function of hematopoietic stem cells by repressing mitochondrial biogenesis and reactive oxygen species. J Exp Med. 2008;205(10):2397-408.

29. Zhen L, Yu L, Dinauer MC. Probing the role of the carboxyl terminus of the gp91phox subunit of neutrophil flavocytochrome b558 using site-directed mutagenesis. J Biol Chem. 1998;273(11):6575-81.

30. Bedard K, Krause KH. The NOX family of ROS-generating NADPH oxidases: physiology and pathophysiology. Physiological reviews. 2007;87(1):245-313.

31. Takahashi K, Yamanaka S. Induction of pluripotent stem cells from mouse embryonic and adult fibroblast cultures by defined factors. Cell. 2006;126(4):663-76.

32. Takahashi K, Tanabe K, Ohnuki M, Narita M, Ichisaka T, Tomoda K, et al. Induction of pluripotent stem cells from adult human fibroblasts by defined factors. Cell. 2007;131(5):861-72.

33. Lin HT, Otsu M, Nakauchi H. Stem cell therapy: an exercise in patience and prudence. Philos Trans R Soc Lond B Biol Sci. 2013;368(1609):20110334.

34. Grskovic M, Javaherian A, Strulovici B, Daley GQ. Induced pluripotent stem cells--opportunities for disease modelling and drug discovery. Nature reviews Drug discovery. 2011;10(12):915-29.

35. Zou J, Sweeney CL, Chou BK, Choi U, Pan J, Wang H, et al. Oxidase-deficient neutrophils from X-linked chronic granulomatous disease iPS cells: functional correction by zinc finger nuclease-mediated safe harbor targeting. Blood. 2011;117(21):5561-72.

36. Jiang Y, Cowley SA, Siler U, Melguizo D, Tilgner K, Browne C, et al. Derivation and functional analysis of patient-specific induced pluripotent stem cells as an in vitro model of chronic granulomatous disease. Stem Cells. 2012;30(4):599-611.

37. Nishimura K, Sano M, Ohtaka M, Furuta B, Umemura Y, Nakajima Y, et al. Development of defective and persistent Sendai virus vector: a unique gene delivery/expression system ideal for cell reprogramming. J Biol Chem. 2011;286(6):4760-71.

38. Suerth JD, Maetzig T, Galla M, Baum C, Schambach A. Self-inactivating alpharetroviral vectors with a split-packaging design. Journal of virology. 2010;84(13):6626-35.

39. Suerth JD, Maetzig T, Brugman MH, Heinz N, Appelt JU, Kaufmann KB, et al. Alpharetroviral self-inactivating vectors: long-term transgene expression in murine hematopoietic cells and low genotoxicity. Mol Ther. 2012;20(5):1022-32.

40. Shibuya K, Shirakawa J, Kameyama T, Honda S, Tahara-Hanaoka S, Miyamoto A, et al. CD226 (DNAM-1) is involved in lymphocyte function-associated antigen 1 costimulatory signal for naive T cell differentiation and proliferation. J Exp Med. 2003;198(12):1829-39.

41. Bonini C, Ferrari G, Verzeletti S, Servida P, Zappone E, Ruggieri L, et al. HSV-TK gene transfer into donor lymphocytes for control of allogeneic graft-versus-leukemia. Science. 1997;276(5319):1719-24.

42. Yamaguchi T, Hamanaka S, Kamiya A, Okabe M, Kawarai M, Wakiyama Y, et al. Development of an all-in-one inducible lentiviral vector for gene specific analysis of reprogramming. PLoS One. 2012;7(7):e41007.

43. Takayama N, Nishimura S, Nakamura S, Shimizu T, Ohnishi R, Endo H, et al. Transient activation of c-MYC expression is critical for efficient platelet generation from human induced pluripotent stem cells. J Exp Med. 2010;207(13):2817-30.

44. Masaki H, Ishikawa T, Takahashi S, Okumura M, Sakai N, Haga M, et al. Heterogeneity of pluripotent marker gene expression in colonies generated in human iPS cell induction culture. Stem cell research. 2007;1(2):105-15.

45. Takayama N, Nishikii H, Usui J, Tsukui H, Sawaguchi A, Hiroyama T, et al. Generation of functional platelets from human embryonic stem cells in vitro via ES-sacs, VEGF-promoted structures that concentrate hematopoietic progenitors. Blood. 2008;111(11):5298-306.

46. Brinkmann V, Laube B, Abu Abed U, Goosmann C, Zychlinsky A. Neutrophil extracellular traps: how to generate and visualize them. Journal of visualized experiments : JoVE. 2010(36).

47. Zhen L, King AA, Xiao Y, Chanock SJ, Orkin SH, Dinauer MC. Gene targeting of X chromosome-linked chronic granulomatous disease locus in a human myeloid leukemia cell line and rescue by expression of recombinant gp91phox. Proc Natl Acad Sci U S A. 1993;90(21):9832-6.

48. Yokoyama Y, Suzuki T, Sakata-Yanagimoto M, Kumano K, Higashi K, Takato T, et al. Derivation of functional mature neutrophils from human embryonic stem cells. Blood. 2009;113(26):6584-92.

49. Brinkmann V, Reichard U, Goosmann C, Fauler B, Uhlemann Y, Weiss DS, et al. Neutrophil extracellular traps kill bacteria. Science. 2004;303(5663):1532-5.

50. Metzler KD, Fuchs TA, Nauseef WM, Reumaux D, Roesler J, Schulze I, et al. Myeloperoxidase is required for neutrophil extracellular trap formation: implications for innate immunity. Blood. 2011;117(3):953-9.

51. Skubitz KM, Campbell KD, Skubitz AP. CD66a, CD66b, CD66c, and CD66d each independently stimulate neutrophils. Journal of leukocyte biology. 1996;60(1):106-17.

52. Kaufmann KB, Brendel C, Suerth JD, Mueller-Kuller U, Chen-Wichmann L, Schwable J, et al. Alpharetroviral vector-mediated gene therapy for X-CGD: functional correction and lack of aberrant splicing. Mol Ther. 2013;21(3):648-61.

53. Ng P, Baker MD. The molecular basis of multiple vector insertion by gene targeting in mammalian cells. Genetics. 1999;151(3):1143-55.

54. Zhang XB. Cellular reprogramming of human peripheral blood cells. Genomics, proteomics & bioinformatics. 2013;11(5):264-74.

55. Pfaff N, Lachmann N, Ackermann M, Kohlscheen S, Brendel C, Maetzig T, et al. A ubiquitous chromatin opening element prevents transgene silencing in pluripotent stem cells and their differentiated progeny. Stem Cells. 2013;31(3):488-99.

56. Li G, Scull C, Ozcan L, Tabas I. NADPH oxidase links endoplasmic reticulum stress, oxidative stress, and PKR activation to induce apoptosis. The Journal of cell biology. 2010;191(6):1113-25.

57. Malhotra JD, Kaufman RJ. Endoplasmic reticulum stress and oxidative stress: a vicious cycle or a double-edged sword? Antioxidants & redox signaling. 2007;9(12):2277-93.

58. Zhen L, King AA, Xiao Y, Chanock SJ, Orkin SH, Dinauer MC. Gene targeting of X chromosome-linked chronic granulomatous disease locus in a human myeloid leukemia cell line and rescue by expression of recombinant gp91phox. Proc Natl Acad Sci U S A. 1993;90(21):9832-6.

59. Tucker KA, Lilly MB, Heck L, Jr., Rado TA. Characterization of a new human diploid myeloid leukemia cell line (PLB-985) with granulocytic and monocytic differentiating capacity. Blood. 1987;70(2):372-8.

60. Uenishi G, Theisen D, Lee JH, Kumar A, Raymond M, Vodyanik M, et al. Tenascin C promotes hematoendothelial development and T lymphoid commitment from human pluripotent stem cells in chemically defined conditions. Stem cell reports. 2014;3(6):1073-84.

61. Herbst F, Ball CR, Tuorto F, Nowrouzi A, Wang W, Zavidij O, et al. Extensive methylation of promoter sequences silences lentiviral transgene expression during stem cell differentiation in vivo. Mol Ther. 2012;20(5):1014-21.

62. Kobayashi SD, Voyich JM, Braughton KR, Whitney AR, Nauseef WM, Malech HL, et al. Gene expression profiling provides insight into the pathophysiology of chronic granulomatous disease. Journal of immunology. 2004;172(1):636-43.

63. Kim SY, Jun HS, Mead PA, Mansfield BC, Chou JY. Neutrophil stress and apoptosis underlie myeloid dysfunction in glycogen storage disease type Ib. Blood. 2008;111(12):5704-11.

64. Hasegawa K, Cowan AB, Nakatsuji N, Suemori H. Efficient multicistronic expression of a transgene in human embryonic stem cells. Stem Cells. 2007;25(7):1707-12.

65. Yoshida LS, Saruta F, Yoshikawa K, Tatsuzawa O, Tsunawaki S. Mutation at histidine 338 of gp91(phox) depletes FAD and affects expression of cytochrome b558 of the human NADPH oxidase. J Biol Chem. 1998;273(43):27879-86.

66. Wu C, Dunbar CE. Stem cell gene therapy: the risks of insertional mutagenesis and approaches to minimize genotoxicity. Frontiers of medicine. 2011;5(4):356-71.

67. Chiriaco M, Farinelli G, Capo V, Zonari E, Scaramuzza S, Di Matteo G, et al. Dual-regulated lentiviral vector for gene therapy of X-linked chronic granulomatosis. Mol Ther. 2014;22(8):1472-83.

68. Miharada K, Sigurdsson V, Karlsson S. Dppa5 improves hematopoietic stem cell activity by reducing endoplasmic reticulum stress. Cell reports. 2014;7(5):1381-92.

69. Halasi M, Wang M, Chavan TS, Gaponenko V, Hay N, Gartel AL. ROS inhibitor N-acetyl-L-cysteine antagonizes the activity of proteasome inhibitors. The Biochemical journal. 2013;454(2):201-8.

70. Cox DB, Platt RJ, Zhang F. Therapeutic genome editing: prospects and challenges. Nature medicine. 2015;21(2):121-31.

71. Hsu PD, Lander ES, Zhang F. Development and applications of CRISPR-Cas9 for genome engineering. Cell. 2014;157(6):1262-78.

72. Genovese P, Schiroli G, Escobar G, Di Tomaso T, Firrito C, Calabria A, et al. Targeted genome editing in human repopulating haematopoietic stem cells. Nature. 2014;510(7504):235-40.

73. Kang EM, Malech HL. Gene therapy for chronic granulomatous disease. Methods in enzymology. 2012;507:125-54.

74. Dodd S, Dean O, Copolov DL, Malhi GS, Berk M. N-acetylcysteine for antioxidant therapy: pharmacology and clinical utility. Expert opinion on biological therapy. 2008;8(12):1955-62.

75. Yamazaki T, Kawai C, Yamauchi A, Kuribayashi F. A highly sensitive chemiluminescence assay for superoxide detection and chronic granulomatous disease diagnosis. Trop Med Health. 2011;39(2):41-5.

76. Assari T. Chronic Granulomatous Disease; fundamental stages in our understanding of CGD. Medical immunology. 2006;5:4.

Acknowledgements

My sincerest gratitude goes to Dr. Makoto Otsu and Professor Hiromitsu Nakauchi for being my mentors, for supervising this work and for giving me the chance to pursue stem cell research in Japan. I would also like to thank Dr. Hideki Masaki and Dr. Tomoyuki Yamaguchi for their teachings in technical skills and general guidance. The technical support of Dr. Yumiko Ishii was invaluable for cell sorting and flow cytometry analyses.

I feel especially grateful towards Mrs. Kimiko Machida. She has provided help and support in so many different ways that it is almost impossible to express my gratitude in words. I would also like to thank Dr. Chen-Yi Lai for her immense generosity and kind-heartedness in offering her time and guidance.

Further gratitude also extends to the numerous collaborators who supported this project. Mr. Yukinori Yatsuda and his team at Bio-Rad kindly collaborated on the ddPCR work. I would also like to thank Dr. Axel Schambach for supplying the alpharetroviral SIN vector. Dr. Manuel Grez and Dr. Kerstin Kaufmann were very generous in offering their technical insight and comments. Additional thanks also goes to Dr. Taizo Wada and Dr. Akihiro Yachie for providing the XCGD patient's peripheral blood sample and Dr. Mahito Nakanishi for providing the Sendai virus vector.

Over the duration of my degree, I have been supported by the Interchange Association of Japan (IAJ) and the Academic Research Grant for Graduate School of Frontier Sciences Doctor Course Students. I have also been supported by the research assistant programs of the excellent graduate schools (EGS), IMSUT, University of Tokyo as well as the Graduate Program in Gerontology, The University of Tokyo Global Leadership initiative for an Age-Friendly Society (GLAFS).

Last but not least, I would like to thank my wife, my son, my parents and the rest of my family for their love and much-valued support.